Atmospheric Environment 141 (2016) 230–244

Contents lists available at ScienceDirect

Atmospheric Environment

journal homepage: www.elsevier.com/locate/atmosenv

Impacts of changes in climate, land use and land cover on atmospheric mercury

H. Zhang [a], C.D. Holmes [b], S. Wu [a, c, *]

[a] Department of Geological and Mining Engineering and Sciences, Michigan Technological University, Houghton, MI 49931, USA
[b] Department of Earth, Ocean and Atmospheric Science, Florida State University, Tallahassee, FL 32306, USA
[c] Atmospheric Sciences Program and Department of Civil and Environmental Engineering, Michigan Technological University, Houghton, MI 49931, USA

HIGHLIGHTS

- We have examined the sensitivities of atmospheric mercury to the changes in climate and land use/land cover.
- Land use and land cover change can lead to increases in Hg(0) dry deposition flux over most of the continental regions.
- Climate change can cause increases in the surface Hg(0) concentration globally.
- Climate change induces significant regional changes in mercury wet deposition.

ARTICLE INFO

Article history:
Received 24 February 2016
Received in revised form
16 June 2016
Accepted 21 June 2016
Available online 22 June 2016

Keywords:
Climate change
Land use/land cover change
Atmospheric mercury
Mercury deposition

ABSTRACT

Mercury is an important pollutant that can be transported globally due to its long lifetime in the atmosphere. Atmosphere-surface exchange is a major process affecting the cycling of mercury in the global environment and its impacts on food webs. We investigate the sensitivities of the air-surface exchange, atmospheric transport, and budget of mercury to projected 2000–2050 changes in climate and land use/land cover with a global chemical transport model (GEOS-Chem). We find that annual mean Hg(0) dry deposition flux over land could increase by up to 20% in northern mid-latitudes by 2050 due to increased vegetation and foliage density. Climate change can significantly affect both the wet deposition and atmospheric chemistry of mercury. In response to the projected climate change, the annual mean wet deposition flux increases over most continental regions and decreases over most of the mid-latitude and tropical oceans. The annual mean mercury wet deposition flux over northern and southern high latitudes increases by 7% and 8% respectively, largely driven by increases in precipitation there. Surface Hg(0) is predicted to increase generally, because high temperatures decrease Hg(0) oxidation by bromine and high moisture increases aqueous Hg(II) photo reduction. The combined effects of projected changes in climate, land use and land cover increase mercury deposition to the continental biosphere and decrease mercury deposition to the marine biosphere.

1. Introduction

Mercury is a toxic and bioaccumulative pollutant in the environment and has important implications for public health, wildlife and ecosystems (Choi and Grandjean, 2008; Lindberg et al., 2007; Mergler et al., 2007; Scheulhammer et al., 2007; UNEP, 2013). The long atmospheric lifetime of elemental mercury (around one year) enables it to be transported long distances before depositing to the Earth's surfaces, making it a global pollutant (Lindqvist and Rodhe, 1985; Schroeder and Munthe, 1998). Due to its volatility, some of the deposited mercury can be emitted back into the atmosphere (Selin et al., 2008; Xu et al., 1999).

The atmosphere-surface exchange and budget of atmospheric mercury are affected by global changes in anthropogenic emissions, climate and land use/land cover. Most previous studies of global change have focused on the effects of anthropogenic emissions and their implications for policy. For example, Corbitt et al. (2011) studied the source-receptor relationship for mercury deposition with the present-day and 2050s anthropogenic emissions. Amos et al. (2013) first investigated the impacts of legacy mercury

* Corresponding author. Department of Geological and Mining Engineering and Sciences, Michigan Technological University, Houghton, MI 49931, USA.
E-mail address: slwu@mtu.edu (S. Wu).

http://dx.doi.org/10.1016/j.atmosenv.2016.06.056
1352-2310/

emissions on the present-day mercury cycle and then projected the effects from future changes in anthropogenic mercury emissions. Selin (2014) identified the challenges for meeting the goals of the Minamata Convention to regulate anthropogenic mercury emission and evaluating its influences on global biogeochemical cycling of mercury. Few studies have addressed the effects of changing climate or land use/land cover on atmospheric mercury. Lei et al. (2014) found that the benefits from reductions in the domestic United States mercury emissions for the 2000–2050 period would be largely offset by rising anthropogenic emissions overseas and rising natural emissions. Megaritis et al. (2014) investigated the effects of climate change on atmospheric mercury concentration and deposition over the eastern United States and concluded that rising future temperatures would increase elemental mercury oxidation and increase divalent mercury concentrations. Hansen et al. (2015) studied the impacts of climate change on atmospheric mercury deposition in the Arctic following the Special Report on Emissions Scenarios (SRES-A1B) (Nakicenovic et al., 2000) as a sensitivity study and found that climate change would reduce atmospheric mercury deposition to the Arctic.

Climate change has the potential to influence atmospheric mercury through multiple pathways. The changes in precipitation directly affect the spatiotemporal patterns of mercury wet deposition. Past studies have shown that the variability in precipitation plays a critical role in affecting the present-day mercury wet deposition (Gratz et al., 2009; Holmes et al., 2016; Nair et al., 2013; Prestbo and Gay, 2009; Risch et al., 2012b). The observed significant interannual variability in present-day atmospheric mercury deposition (Blackwell et al., 2014) also indicates that meteorology is a key factor affecting the atmospheric abundance, distribution and atmosphere-surface exchange of mercury.

Changes in temperature could alter the atmospheric mercury chemistry leading to changes in mercury speciation (i.e. elemental vs. divalent mercury; gas vs. particle phase) and consequently deposition since different mercury species have different solubility and other deposition properties. The changes in future climate could also affect the atmosphere-surface exchange of elemental mercury. Previous studies have shown that evasion of mercury from surface soil could be affected by solar radiation (Eckley and Branfireun, 2008; Ericksen et al., 2006; Fu et al., 2012b; Gustin et al., 2006; Obrist et al., 2006) and air temperature (Almeida et al., 2009; Obrist et al., 2006; Poissant et al., 1999). Emission of mercury from the surface ocean can also be affected by environmental factors such as temperature, solar radiation and surface winds (Andersson et al., 2008; Nightingale et al., 2000; Poissant et al., 2000; Soerensen et al., 2010, 2013, 2014).

Significant changes in land use/land cover are expected in the coming decades in response to changes in climate, atmospheric CO_2 concentration, as well as anthropogenic activities such as agriculture expansion, deforestation and reforestation (Bachelet et al., 2001; Cox et al., 2004; Cramer et al., 2001; Houghton et al., 2000; Turner et al., 1994). Previous work has investigated the influence of land use/land cover change on atmospheric chemical composition such as ozone (Ganzeveld et al., 2010; Wu et al., 2012), but the potential impacts on atmospheric mercury from changes in land use/land cover have not been examined yet. Recent assessments have suggested vegetation to be a net sink of atmospheric mercury (Ericksen and Gustin, 2004; Gustin et al., 2008; Hanson et al., 1995; Hartman et al., 2009; Wang et al., 2014). Strong positive correlations between mercury deposition flux and leaf area have been indicated by studies of Gao and Wesely (1995) and Zhang et al. (2009). Zhang et al., (2009) showed that the Hg(0) dry deposition velocity onto forests tended to be 2–5 times higher than other vegetated surfaces. We present here the first study on the impacts of global climate change and land use/land cover change (driven by climate change, increasing atmospheric CO_2 concentration and agricultural land use change) on atmospheric mercury.

2. Model description and approach

2.1. Model description

We use the GEOS-Chem model version v9-02 (www.geos-chem.org) with a coupled atmosphere-land-ocean mercury simulation (Holmes et al., 2010; Selin et al., 2008; Soerensen et al., 2010). The model simulates three forms of mercury in the atmosphere: gaseous elemental Hg(0), gaseous oxidized Hg(II) and particle-bound Hg(II). Hg(II) is assumed to be in equilibrium between gas and particle phases at all times and the fractions in gas and particle phases depend on temperature and aerosol loadings (Amos et al., 2012; Rutter and Schauer, 2007a, b). Atmospheric Hg(0) is oxidized by bromine (Br) to form Hg(II) products and in-cloud reduction of Hg(II) is also included in order to match observed surface mercury concentrations (Holmes et al., 2010). The oxidation of Hg(0) involves a two-step reaction: (1) atmospheric Hg(0) reacts with Br to form unstable HgBr; (2) HgBr can either dissociate or react with Br or the hydroxyl radical ($^{\cdot}OH$) to form the final product (Hg(II)) (Holmes et al., 2010). Tropospheric Br fields for the present-day are archived from a GEOS-Chem full chemistry simulation (Parrella et al., 2012) and remain unchanged in our future climate and land use/land cover simulations. Gaseous and particle-bound Hg(II) are subject to wet deposition, which includes scavenging in convective updrafts and rainout and washout from large-scale precipitation as described in Liu et al. (2001) with updates by Wang et al. (2011) and Amos et al. (2012). Sea salt uptake of gaseous phase Hg(II) in the marine boundary layer (MBL) is accounted for, as described by Holmes et al. (2010).

Hg(0) is emitted from both natural and anthropogenic sources while Hg(II) only has anthropogenic sources. Anthropogenic emissions are specified from the GEIA (Global Emission Inventories Activity) 2005 inventory (Pacyna et al., 2010) as implemented by Corbitt et al. (2011) and Streets et al. (2009). Anthropogenic emissions over the United States and Canada are replaced by regional inventories prepared by Zhang et al. (2012b). Anthropogenic mercury emissions are held constant in our future modeling scenarios in order to focus on the effects of climate and land use/land cover on natural emissions and atmospheric chemistry.

The atmosphere-terrestrial exchange of Hg(0) is bi-directional, but only some recent model developments have coupled the deposition (downward flux) and emission (upward flux) to estimate the net atmosphere-surface flux based on the gradient between an ambient mercury concentration and a “compensation point” inferred from the surface characteristics (Bash et al., 2007; Bash, 2010; Wang et al., 2014). Such treatments have not been implemented into global chemical transport models yet due to the limited field or lab data to validate the complicated parameterization processes in the coupled model (Wang et al., 2014). The GEOS-Chem model used in this study treats deposition and emission of Hg(0) separately. More details about the dry deposition process will be discussed in Sec 2.2.

A fraction of Hg(II) deposited to the terrestrial reservoir can be quickly converted to Hg(0) and reemitted to the atmosphere, which is called “prompt recycling” (Selin et al., 2008). For the version of GEOS-Chem used in this study, it is assumed that 20% of total Hg(II) deposited to the land surface will be immediately released to the atmosphere as Hg(0) when there is no snow cover (Selin et al., 2008). For snow covered land surfaces, a snow pack reservoir accounts for the conversion of deposited Hg(II) to Hg(0) under sunlit conditions (Holmes et al., 2010). The reservoir lifetime is 180 days but decreases to 21 days when temperature exceeds 270 K (Fain

et al., 2007, 2008).

Dry deposition of Hg(0) to the ocean surface in GEOS-Chem is simulated as part of the bi-directional exchange process in the surface slab ocean model of Soerensen et al. (2010). In this model, three species of mercury in the surface ocean mixed layer are simulated: Hg(0), Hg(II) and nonreactive nonvolatile mercury. Atmospheric deposition of mercury contributes significantly to the surface ocean mixed layer, but the deep ocean also accounts for a considerable amount of mercury inputs to the surface ocean mixed layer. Vertical exchange between the surface ocean and the deep ocean are retained through entrainment/detrainment and Ekman pumping (Soerensen et al., 2010). In the surface ocean mixed layer, biological primary productivity and solar radiation both favor Hg(II) reduction to Hg(0). Net emission of Hg(0) from the surface ocean is a function of sea surface temperature, surface wind speed and the available Hg(0) in the surface ocean. Net emission of Hg(0) from the surface ocean is estimated to be about 2310 Mg yr^{-1} for present-day in this study, which is consistent with most other estimates of 2000–3000 Mg yr^{-1} (Bergan et al., 1999; Holmes et al., 2010; Lindberg et al., 2007; Mason and Sheu, 2002; Seigneur et al., 2004; Selin et al., 2007; Shia et al., 1999; Soerensen et al., 2010).

2.2. Simulation design

All the model simulations are driven by meteorology fields archived from the NASA Goddard Institute for Space Studies (GISS) general circulation model (GCM 3) (Rind et al., 2007). The GISS GCM 3 has a horizontal resolution of 4° latitude by 5° longitude with 23 vertical layers extending from the surface to 0.002 hPa (about 85 km altitude). The meteorological data is archived with 6-hour time resolution (3-hour for surface variables and mixing depth). The interface between the GISS GCM 3 and GEOS-Chem is described in Wu et al. (2007). The simulation of 2000–2050 climate change with the GISS model follows the IPCC A1B scenario (IPCC, 2001). We carry out 5-year Hg simulations with the GEOS-Chem model for the 2000s (1998–2002) and 2050s (2048–2052) climate. Unless noted otherwise, our analyses on the perturbations to atmospheric mercury due to climate change are based on 5-year average model results.

We follow Wu et al. (2012) to conduct GEOS-Chem sensitivity simulations to separately identify the effects of climate change, natural vegetation change (also referred to as land cover change here) induced by climate change and increasing atmospheric CO_2 fertilization, and anthropogenic land use change such as agricultural expansion (also referred to as land use change here). The 2000–2050 changes in natural vegetation are calculated with the Lund-Potsdam-Jena Dynamic Global Vegetation Model (LPJ DGVM) (Sitch et al., 2003) driven by the same meteorology from the GISS GCM 3 and atmospheric CO_2 concentrations following the IPCC A1B scenario (IPCC, 2001). Changes in anthropogenic land use over the period of 2000–2050 were simulated by the IMAGE model following the IPCC A1B scenario (IMAGE-Team, 2001; IPCC, 2001; MNP, 2006).

The LPJ DGVM simulates vegetation cover, density and other variables for nine different plant functional types (PFTs) (Sitch et al., 2003; Wu et al., 2012). Vegetation data including vegetation density (expressed as leaf area index, or LAI) and fractional coverage from LPJ are archived at 1° × 1° (longitude × latitude) resolution. We use 10-year average vegetation data to derive the 2000–2050 changes in land use/land cover (1990–2000 for the present-day and 2040–2050 for the future). Dry deposition of Hg(0) and gas phase Hg(II) follows a standard resistance-in-series scheme (Wang et al., 1998; Wesely, 1989) with updates to include the impacts of LAI on stomatal resistance (Gao and Wesely, 1995). Dry deposition velocities for each grid box are calculated with surface values of momentum and sensible heat flux, temperatures, solar radiation and other meteorology variables (Bey et al., 2001).

We conduct five model simulations to separate the impacts associated with climate change and those associated with land use/land cover change: (1) present-day climate and present-day land use and land cover (2000 climate + 2000 LU&LC), (2) future climate and present-day land use and land cover (2050 climate + 2000 LU&LC), (3) present-day climate and future land use and land cover (2000 climate + 2050 LU&LC), (4) present-day climate and present-day land cover (with only natural vegetation) (2000 climate + 2000 LC), (5) present-day climate and future land cover (with only natural vegetation) (2000 climate + 2050 LC). In simulations (4) and (5), only natural vegetation is included while anthropogenic land use such as crops is excluded. Anthropogenic, biomass burning and geogenic emissions of mercury remain at the present-day levels for all the cases, while ocean and land emissions respond dynamically to changes in climate and land use/land cover. The climate-induced changes in temperature, precipitation, cloudiness, and atmospheric transport can all affect atmospheric mercury. In this study, we do not account for the potential impacts from climate change on net primary productivity and wind-driven Ekman pumping. Case (1) serves as the control run and the difference between case (2) and case (1) reflects the influence from climate change. The difference between (4) and (5) represents the impacts from land cover change while the difference between (3) and (1) shows the impacts from the combined effects from land use and land cover. Following Selin et al. (2008), steady state of emissions and deposition on the 4° × 5° model grid is applied to compute natural soil mercury concentrations in preindustrial conditions. For the present-day, soil mercury concentrations are increased by 15% globally (Mason and Sheu, 2002) and distributed following the pattern of present-day anthropogenic deposition. For the present-day simulations, each scenario covers a five-year period (i.e. 1998–2002 or 2048–2052) which is preceded by 5 years of spin-up. All the results analyzed and discussed in this study are based on 5-year averages.

3. Results and discussions

3.1. Model evaluation

Mercury simulations with the GEOS-Chem model driven by the NASA/GEOS assimilated meteorological fields have been extensively evaluated in previous studies (Amos et al., 2012; Holmes et al., 2010; Selin et al., 2007; Soerensen et al., 2010; Song et al., 2015; Strode et al., 2007; Zhang et al., 2012b). In this study, we first evaluate the GEOS-Chem mercury simulations driven by GISS GCM 3 meteorological fields. Fig. 1 shows the simulated concentrations of total gaseous mercury (TGM = Hg(0) + gas phase Hg(II)) in surface air compared with observations. In general, the model reproduces the spatial distribution of atmospheric mercury at 39 continental sites ($r^2 = 0.78$) although it tends to underestimate the TGM surface concentrations. The model calculated mean and standard deviation (SD) for atmospheric mercury concentrations over these sites is 1.52 ± 0.25 ng/m^3, compared to the observed 1.86 ± 0.99 ng/m^3. One likely reason for the underestimate of the surface TGM concentration in our model is the relatively coarse vertical resolution in the boundary layer (0.4 km), which is unable to resolve vertical TGM gradients in strong emission regions, where many TGM measurements are made.

Fig. 2 shows the model calculated annual average wet deposition flux for the present-day (1998–2002) compared with measurements from the Mercury Deposition Network (MDN) (NADP, 2009) over North America. The model simulates the magnitude of wet deposition flux reasonably well with a mean bias of −5% relative to the MDN observational data with correlation of $r^2 = 0.26$.

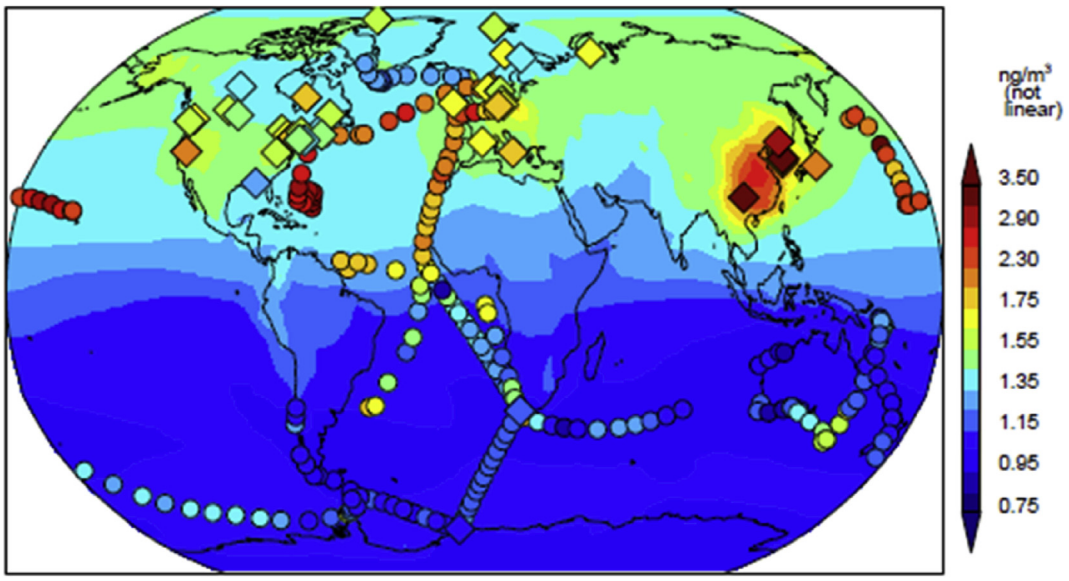

Fig. 1. Global distribution of TGM concentrations in surface air. Model results (background) are annual average for year 1998–2002. Measurements (diamonds) and all other observed ship cruise data (circles) are those used from Holmes et al. (2010).

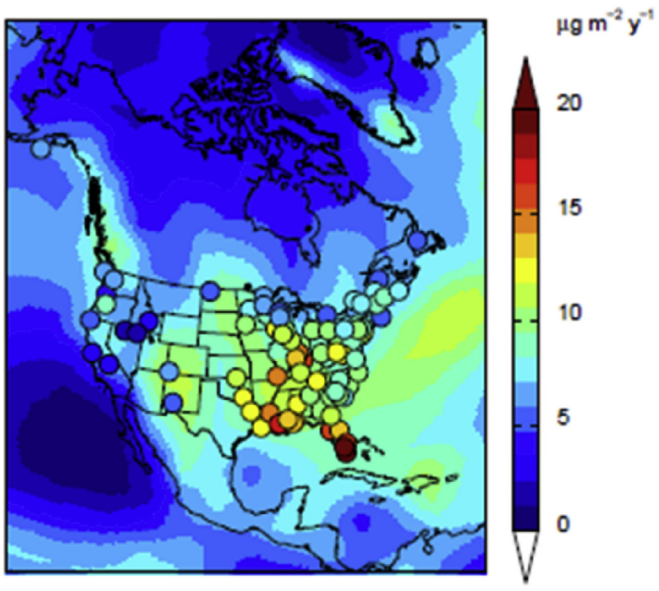

Fig. 2. Annual average total mercury (gas phase Hg(II) + particulate phase Hg(II)) wet deposition flux (in μg/m^2/yr) over North America. Model results (background) for 1998–2002 annual average are compared to observed data from the Mercury Deposition Network (circles) from 2006 to 2008 as used in (Holmes et al., 2010). More details about the data can be found in (Holmes et al., 2010).

The model overestimates the wet deposition flux in the southwestern United States. This could be partly driven by the overestimated precipitation by the GISS CCM 3. For example, we find that at one site in New Mexico (NM10), the precipitation from GISS GCM 3 is 2.4 times higher than the observed precipitation from MDN while the model simulated wet deposition at that site is 83% higher than the measurement from MDN. The modelled largest mercury wet deposition flux is found in the southeastern United States as in other studies (Holmes et al., 2010; Selin and Jacob, 2008; Zhang et al., 2012b; Zhang and Jaegle, 2013) but the model did not capture the magnitude of the observed wet deposition flux with a mean bias of −30% relative to the measured data. Convective scavenging of mercury from the free troposphere very likely contributes to the regional feature (Selin and Jacob, 2008; Zhang et al., 2012b).

The present-day global mercury burden in the atmosphere is estimated to be 4840 Mg yr^{-1}, which is in the range of 4600–5600 Mg yr^{-1} as estimated by other studies (Amos et al., 2012; Selin, 2009; Shia et al., 1999). Mercury emission from geogenic sources follows Selin et al. (2007) with a global total of 500 Mg yr^{-1} and is assumed to remain constant in the future. Biomass burning emission of mercury is estimated to be 243 Mg yr^{-1} following the distribution of Global Fire Emissions Database version 3 (van der Werf et al., 2010) of CO with a constant Hg/CO ratio of 100 nmol mol^{-1} (Holmes et al., 2010). The mercury emission from soil is affected by solar radiation following Holmes et al. (2010) and Zhang et al. (2001) with the global total emission calculated to be 814 Mg yr^{-1} for the present-day.

We calculate 241 Mg yr^{-1} and 204 Mg yr^{-1} re-emission of Hg(0) from the non-snow covered and snow covered land surface respectively. We define net emission of Hg(0) from the terrestrial surface as total Hg(0) emissions from the terrestrial surface minus total Hg(0) dry deposition to the terrestrial surface, i.e. (soil emission + biomass burning emission + geogenic emission + prompt recycling emission − dry deposition). We then calculate the net emission of Hg(0) from the terrestrial surface for present-day is 500 Mg yr^{-1}, lower than the previous bottom-up estimates 1140–5280 Mg yr^{-1} of Mason (2009) and Pirrone et al. (2010). It is lower than the average of 1070 Mg yr^{-1} (uncertainty range: −510 to 3130 Mg yr^{-1}) of Song et al. (2015) from a standard GEOS-Chem simulation and the major uncertainty there comes from the estimation of soil emission (1680 ± 840 Mg yr^{-1}), while it is close to the average of 340 Mg yr^{-1} (uncertainty range: −590 to 1750 Mg yr^{-1}) from GEOS-Chem simulations with optimized emission/parameters based on Bayesian inversion of Song et al. (2015). The recent work of Agnan et al. (2016) estimated a global net emission of Hg(0) from the terrestrial surface to have a median of 607 Mg yr^{-1} with an uncertainty range of−513 Mg yr^{-1}, 1653 Mg yr^{-1} (representing 37.5th and 62.5th percentile range) by extrapolating the best statistical distribution of measurement fluxes from different land cover types and surfaces.

Previous studies (Zhang et al., 2009, 2012a) have shown that

Hg(0) dry deposition velocity values are larger over ecosystem with larger LAI due to the dominant effect of LAI, and gaseous Hg(II) has a much larger dry deposition velocity than Hg(0). Here, the calculated Hg(0) dry deposition velocity ranges from 0.01 cm/s to 0.05 cm/s globally with higher values (0.03–0.05 cm/s) over vegetated areas such as the southeastern United States, the Amazon forest and northern mid-latitudes. The gaseous Hg(II) dry deposition velocity is estimated to range from 0.06 to 5 cm/s globally in this work. These calculated values are well within the range reported by previous studies (Zhang et al., 2009, 2012a). The annual mean Hg(0) dry deposition flux in the central and eastern United States from this work ranging from 11 to 20 μg/m^2/yr are in the range of Zhang et al. (2012a) which estimated Hg(0) dry deposition flux to be 5.2–34.4 μg/m^2/yr at sites in this region, obtaining good agreement with litterfall measurements (Risch et al., 2012a). The global total Hg(0) dry deposition to the land of 1440 Mg for present-day is well within the previous published data (Holmes et al., 2010; Selin et al., 2008; Song et al., 2015). Comparison to the results of these studies suggests that model estimates for Hg(0) dry deposition in this study are reasonable.

3.2. Effects on atmospheric chemistry and composition

Bromine reactions with Hg(0) are very sensitive to air temperature, with the net oxidation rate falling roughly 11% for each 1 K increase in temperature (Holmes et al., 2006). Fig. 3 shows the zonal mean gross oxidation of Hg(0) for present-day and the difference due to 2000–2050 climate change. Bromine concentrations are assumed to be the same in the future climate since little is known about how its marine sources may change (Hossaini et al., 2013; Hughes et al., 2012). The higher tropospheric temperatures in the future climate favor decomposition of the HgBr reaction intermediate and therefore suppress oxidation of Hg(0) to Hg(II) (Fig. 3). Although the mechanism for atmospheric reduction of Hg(II) is uncertain, numerous studies have suggested that aqueous photochemical reactions in clouds or aerosols are involved (Lin et al., 2006; Subir et al., 2011, 2012). Rising atmospheric temperatures in the future climate expand the regions where liquid-water clouds exist at higher latitudes and altitudes. Our model therefore predicts 5% greater Hg(II) reduction in the future climate. The interannual variability (IAV, calculated as standard deviation of annual mean values) in present-day Hg(II) reduction is 16 Mg yr^{-1}, which is 0.9% of the mean. In the future scenario, the IAV rises to 27 Mg yr^{-1}, which is 1.4% of the future mean. Against this low IAV, the simulated 5% increase in Hg(II) reduction is significant. Despite the uncertainties associated with the current atmospheric mercury redox chemistry (Holmes et al., 2006, 2010; Lin et al., 2006; Pongprueksa et al., 2008; Subir et al., 2011, 2012), our results suggest that climate change could lead to large perturbations to atmospheric mercury chemistry.

The change in future temperature could have potential effects on the partitioning of Hg(II) between the gas and particulate phase. Amos et al. (2012) has shown that implementing the partitioning of Hg (II) between the gas and particulate phase in GEOS-Chem model has resulted in Hg(II) fraction in the particulate phase from less than 10% in warm air with low aerosol and more than 90% in cold air with high aerosol load. This feature is reflected in our model results for the present-day conditions as shown in Fig. 4. The increase in global surface temperature by about 2 K in the future favors more Hg(II) in the gas phase over the particulate phase in most parts of the world (Fig. 4) with the mean fraction of Hg(II) partitioned into the particle phase decreasing by 5% globally in both January and July. This would have important impacts for mercury speciation and subsequent effects on global distribution of mercury deposition. Particulate Hg(II) can be more efficiently scavenged by snow than gaseous Hg(II) (Amos et al., 2012; Holmes et al., 2010; Selin et al., 2008). One important implication could be the influence on mercury deposition in the high latitudes as suggested by Amos et al. (2012) which showed that the implementation of the partitioning relationship leads to increasing Hg(II) deposition at high latitudes comparing to a sensitivity simulation that assumes all Hg(II) to be in the gaseous phase. The model results predict that future climate could cause the fraction of Hg(II) in the particulate phase to decrease by 45% and 5% in January in northern (Arctic Ocean) and southern (Antarctic Ocean) high latitudes (poleward of 70°N and 65°S), mainly driven by the increase in surface air temperature in these two regions, while no significant change is found in July in both high latitudes. We find here that particle phase Hg(II) concentration decreases in high latitudes in both hemispheres affected by the gas phase partitioning and also the increase in precipitation over high latitudes.

We find that climate change leads to a general increase in future surface Hg(0) concentrations by up to 5% and 7% in the northern and southern hemispheres respectively mainly as a combined result of suppressed Hg(0) oxidation in the troposphere and increased in-cloud reduction of Hg(II) (Fig. 5). The largest increase by up to 0.14 ng/m^3 occurs in eastern China where the present-day surface Hg(0) concentration in urban sites are often several folds higher than that of those in North America and Europe (Fu et al., 2012a). We further divide the continental regions into North

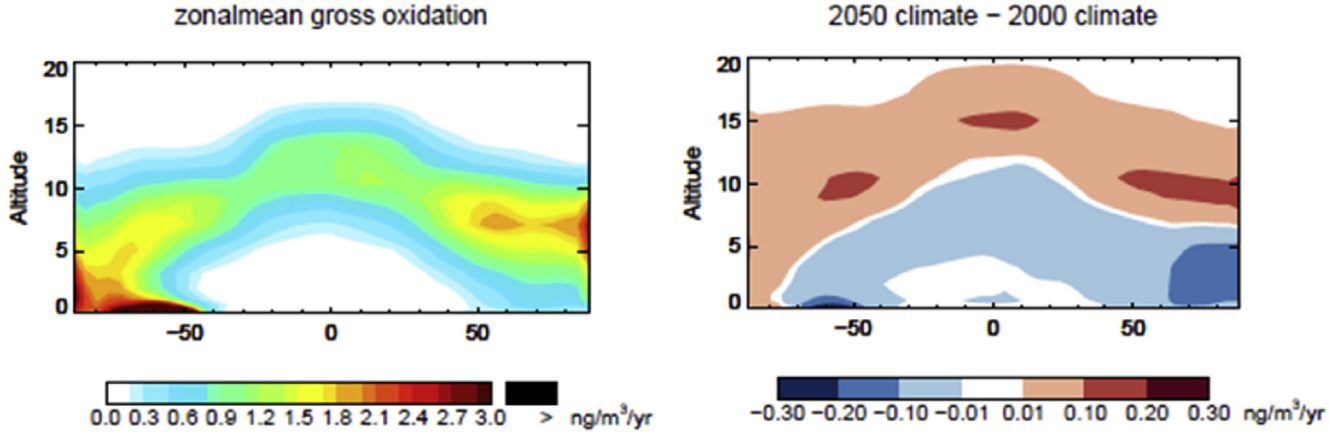

Fig. 3. Zonal mean gross oxidation of Hg(0) (left) and the difference due to 2000–2050 climate change (right).

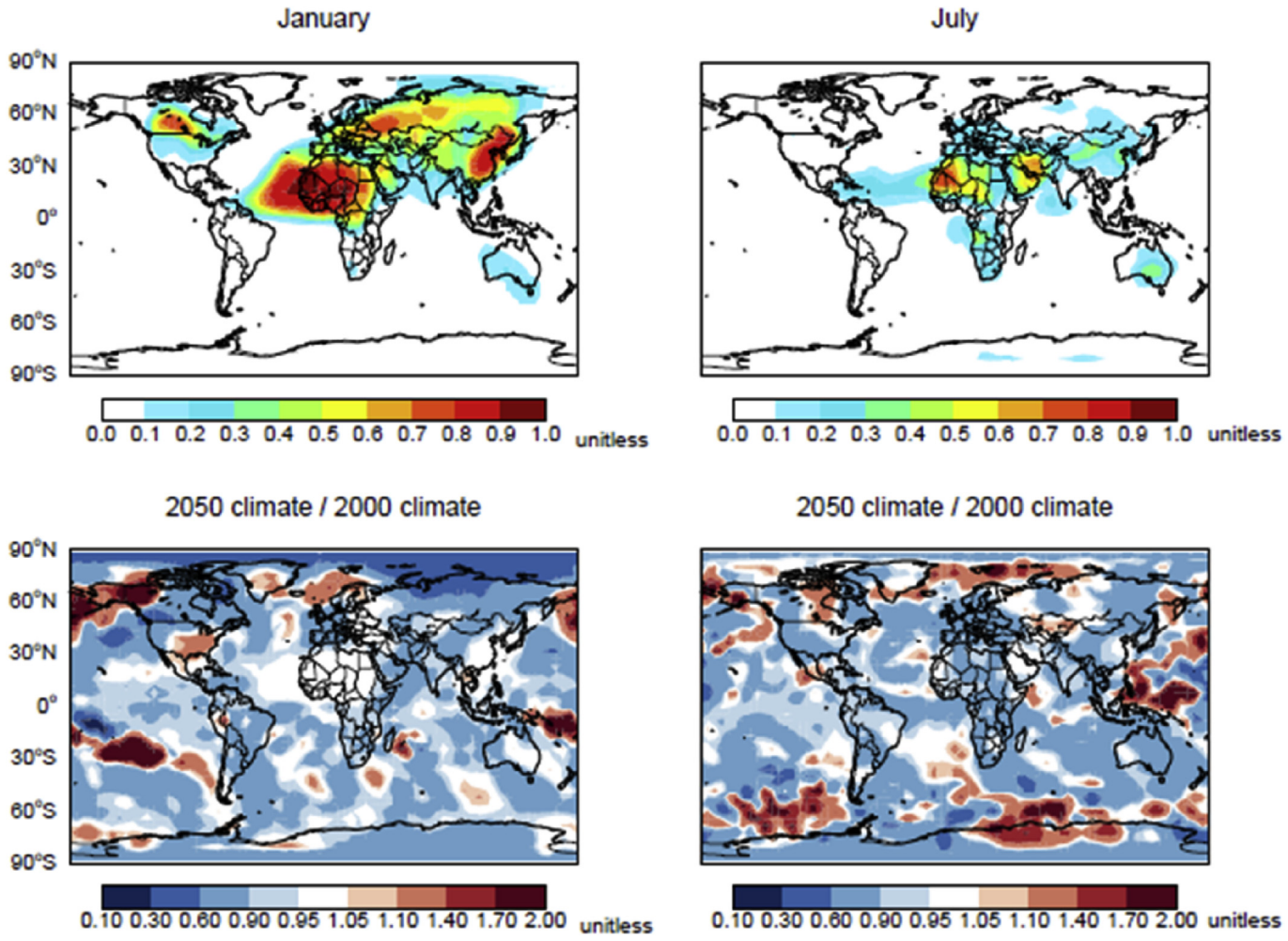

Fig. 4. Top panels are the mean fraction of Hg(II) partitioned into the particle phase in surface air in January (top left) and July (top right). Bottoms are the respective ratio due to 2000–2050 climate change.

America (130–80°W and 10–70°N), Europe (10°W–50°E and 35–70°N), Asia (63–145°E and 10–58°N), Africa (15°W–50°E and 35°S–35°N), South America (80–40°W and 55°S–10°N) and Australia (115–150°E and 35–15°S) shown as the red boxes in the bottom right of Fig. 5. We find climate change causes the annual average surface Hg(0) concentration to increase by 4%, 4%, 3%, 5%, 5% and 7% in the respective regions and these changes are statistically significant at the 95% confidence level. Unless noted otherwise, the standard error of the mean and confidence levels from two-sample *t*-test is applied and also accounts for serial correlation in the annual means of the simulation (Wilks, 2006). The IAV of surface Hg(0) concentration is about 0.01 ng/m^3 (1% of the mean) over most of the regions in the present-day showing the longer lifetime of atmospheric Hg(0). At the same time, the average surface air Hg(0) concentration in northern and southern high latitudes under the future climate scenario increases by 5% and 7% respectively and these increases are significant at the 95% confidence level. This is similar to that of Hansen et al. (2015) which predicted a 4% higher average Arctic air concentration of Hg(0) in the future climate. In addition, our model results here show that the annual mean surface Hg(0) concentration over the United States will increase by 0.05–0.07 ng/m^3 in the future climate. A previous study by Megaritis et al. (2014) predicted that climate change following the IPCC A2 scenario would slightly decrease the Hg(0) level by up to 0.07 ng/m^3 in summer and less in winter (<0.01 ng/m^3) over the eastern United States, but the atmospheric chemistry including both gaseous phase and aqueous phase oxidation in the model is different from the chemistry in the current model. In contrast, 2000–2050 changes in land use/land cover both individually and together lead to a decrease in the Hg(0) concentration as a result of the enhanced uptake of Hg(0) by vegetation. Land use and land cover together could drive the surface Hg(0) concentration to a decrease by 3% at the 95% confidence level in the northern hemisphere although little change was found for the southern hemisphere. The larger decrease in the northern hemisphere reflects the higher vegetation coverage in the northern hemisphere, especially the northern mid-latitudes.

The changes in the surface Hg(II) concentration shows greater spatial variability than Hg(0), reflecting the shorter lifetime of Hg(II) (Fig. 6). The surface average gaseous phase Hg(II) concentration over North America is calculated to decrease by 16% due to the increase in wet deposition. We also find climate change causes the surface gas phase Hg(II) concentration to decrease by 34% and 17% significantly over northern and southern high latitudes while no significant changes are found in these regions driven by future land use/land cover change. The decrease is a result of the change in atmospheric chemistry and wet deposition over the high latitudes in the future climate (Hansen et al., 2015). We also found a 41%

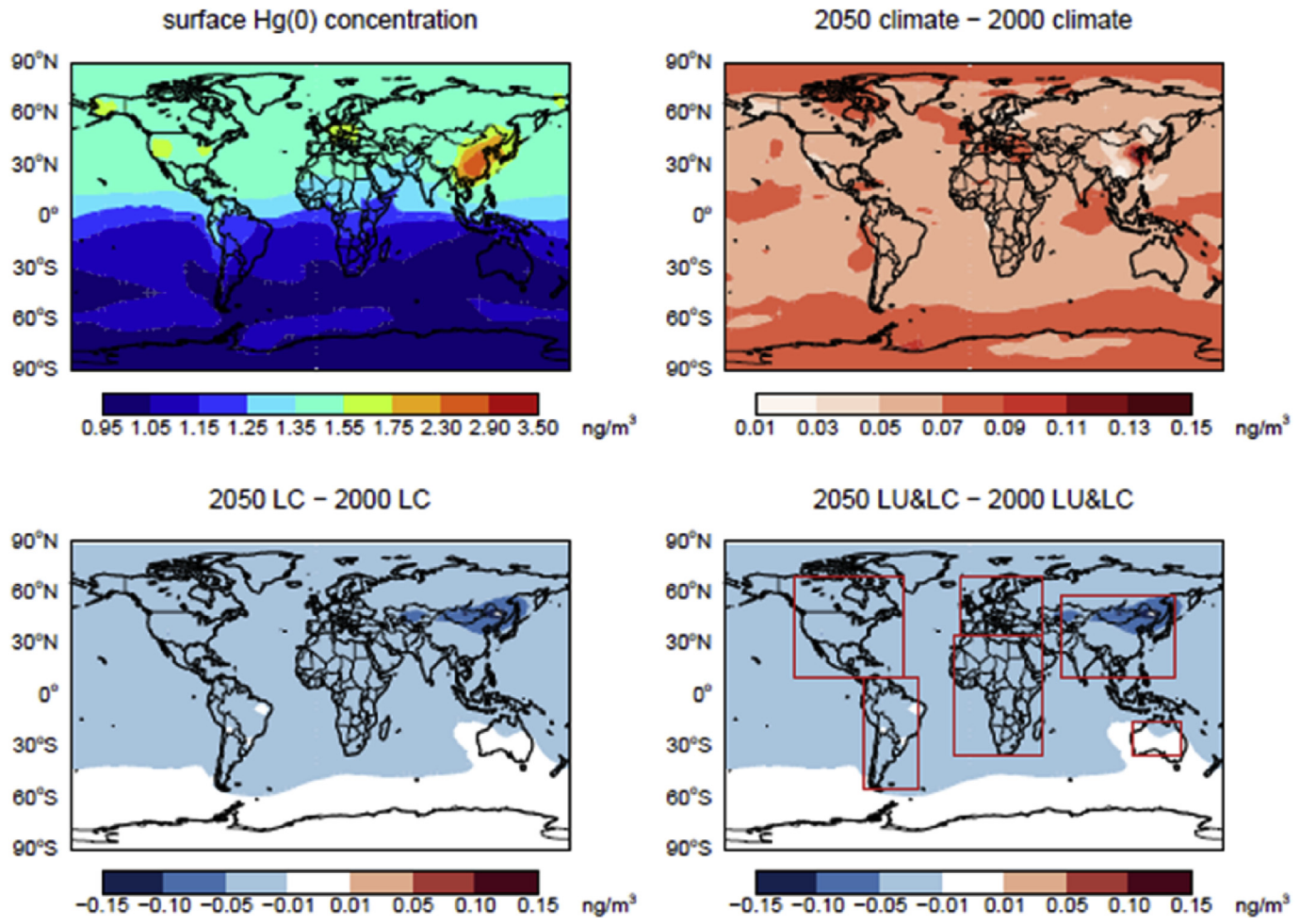

Fig. 5. Annual mean surface Hg(0) concentration for the present-day (top left) and the difference due to 2000–2050 climate change (top right), 2000–2050 land cover change (bottom left), 2000–2050 land use/land cover change (bottom right).

decrease in the surface average Arctic air concentration of RGM (equivalent to gas phase Hg(II) in the present study) in the future climate. The surface gaseous phase Hg(II) concentration is calculated to decrease by 10%, 31%, 7% and 10% in the North Pacific (defined as 180–80°W, 25–180°E and 30–70° N), North Atlantic (defined as 80–25° W and 55–70°N), Middle Atlantic (defined as 80–25° W and 25°S–55°N) and South Atlantic (defined as 80–25° W and 65°–25°S), respectively. The decreases are driven by increases in precipitation and suppressed Hg(0) oxidation in the troposphere. In contrast, land use/land cover changes drive the surface average gas phase Hg(II) concentration to decrease by 4% and 12% in South America and Australia respectively, largely driven by the increase in Hg(II) dry deposition and these changes are significant at the 95% confidence level.

3.3. Effects on the air-surface exchange of mercury

Air-surface exchanges, including emissions and deposition, are important processes affecting the circulation and distribution of mercury in the global environment. Fig. 7 shows the model calculated annual mean Hg(0) dry deposition flux for present-day and the perturbations due to 2000–2050 changes in climate and land use/land cover, individually and together. The changes in future climate alone cause a general increase in the annual mean Hg(0) dry deposition flux in most of the continental regions by up to 1.0 $\mu g/m^2/yr$ (the IAV ranges from 0.06 to 0.2 $\mu g/m^2/yr$). We find the climate-induced change in the global annual average Hg(0) dry deposition velocity is negligible and therefore the increases in Hg(0) dry deposition flux are mainly driven by the increases in surface Hg(0) concentrations as discussed in Sec 3.2.

Projected 2000–2050 vegetation changes alone increase the annual mean Hg(0) dry deposition flux in most parts of Northern mid-latitudes, North Africa, Northern Australia and the southern part of South America (bottom left panel in Fig. 7). We find large increases in the annual mean Hg(0) dry deposition flux by up to 6 $\mu g/m^2/yr$ in the western United States, part of North Africa, central Asia and northern China. This change is driven by a 50–80% increase in Hg(0) dry deposition velocity over denser vegetation in the future, which is caused by CO_2 fertilization and climate change. As discussed in Wu et al. (2012), some conifer forests dominated by needle leaf trees are expected to be replaced by temperate forests dominated by broadleaf trees following the 2000–2050 natural vegetation change. Globally, it is simulated that the spatial coverage of temperate broadleaf summer green trees will increase by ~20% while boreal needle leaf evergreen trees decrease by ~7%. The most significant changes in vegetation cover are found over northern mid-latitudes, with ~39% increase in temperate deciduous broadleaf trees and ~8% decrease in boreal evergreen needle leaf trees. Furthermore, general increases in LAI are found everywhere except for the subtropical regions in response to changes in vegetation

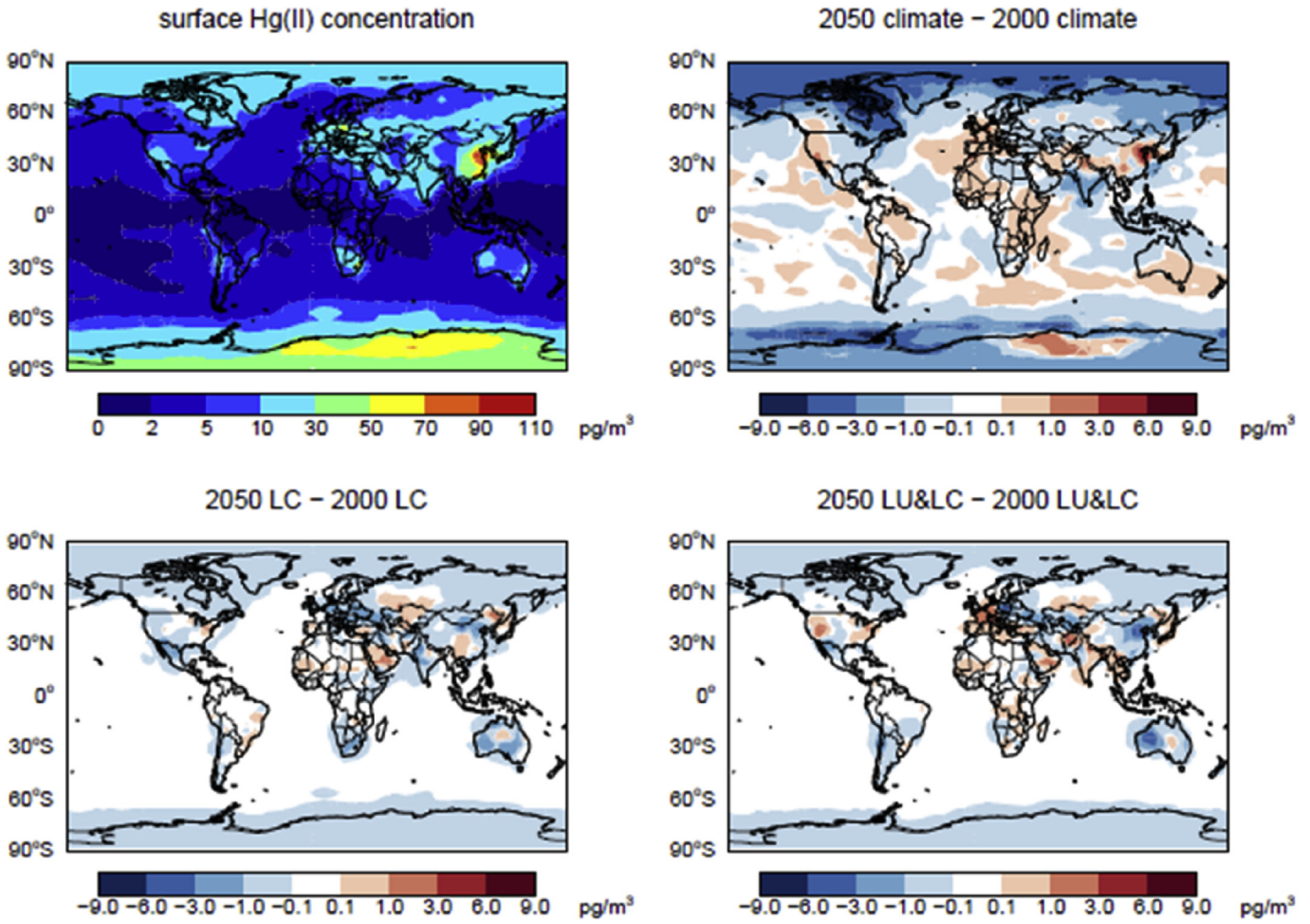

Fig. 6. Same as Fig. 5, but for annual mean surface gaseous phase Hg(II) concentration.

over the 2000–2050 period driven by climate change and CO_2 fertilization. Decreases in Hg(0) dry deposition flux up to 2 μg/m^2/yr are found over the eastern United States, part of the Amazon forest and southern Australia, driven by decreases in LAI. Overall, the surface Hg(0) dry deposition flux is found to increase significantly by 5%, 4%, 4%, and 4% in North America, Europe, Asia and Africa respectively. No significant change is found in South America while a decrease of 34% is found in Australia largely due to the decrease in LAI.

The IPCC A1B scenario (IPCC, 2001; MNP, 2006) projects that agricultural land area will increase over some regions including the eastern United States, South Asia and Central Africa but decrease over East Asia driven by the changes in population, economic development and energy consumption (MNP, 2006). We find that in general the anthropogenic land use change has a smaller impact on mercury deposition when compared to the impact from natural vegetation change (driven by changes in climate and atmospheric CO_2 fertilization). When considering the combined effects from natural vegetation change and anthropogenic land use change, decreases in Hg(0) dry deposition flux over South Asian and middle of central Africa up to 2 μg/m^2/yr are found in response to the decrease in LAI driven by agricultural expansion and deforestation there. The combined effects of land use and land cover cause similar changes in the surface Hg(0) dry deposition flux over North America (+4%), Europe (+3%) and Africa (+5%) compared with that of land cover change alone. The role of vegetation as a source or sink of atmospheric Hg(0) has been in debate, but more recent assessments show that vegetation acts more as a net sink (Ericksen et al., 2003; Hartman et al., 2009; Rutter et al., 2011). Our results here suggest the strong sensitivity of Hg(0) dry deposition to future land use/land cover change in spite of large uncertainties associated with the atmosphere-foliar exchange flux measurements (Agnan et al., 2016; Zhu et al., 2016). It further emphasizes the importance of better constraints on the atmosphere-surface exchange of Hg(0).

Fig. 8 shows the model calculated annual mean total mercury (gaseous phase Hg(II) + particulate phase Hg(II)) wet deposition flux for the present-day and the perturbations due to 2000–2050 climate change as well as the changes in precipitation. The changes in total mercury wet deposition flux are well correlated with the changes in precipitation in the future climate (lower right panel of Fig. 8), with the noticeable exception of the tropical region. With abundant precipitation in the tropical rain belt, wet scavenging is nearly insensitive to the increases in precipitation, so the suppressed oxidation of Hg(0) to Hg(II) leads to decreased wet deposition of Hg(II) in the tropics. We find 6% and 7% increases at the 95% confidence level in annual mean mercury wet deposition flux in Africa and South America while no significant changes are found in North America, Europe, Asia and Australia (present-day IAV of annual mean mercury wet deposition flux is about 2%–3% of the mean). Furthermore, the annual mean mercury wet deposition flux decreases by 3% in the Middle Atlantic while the changes in the

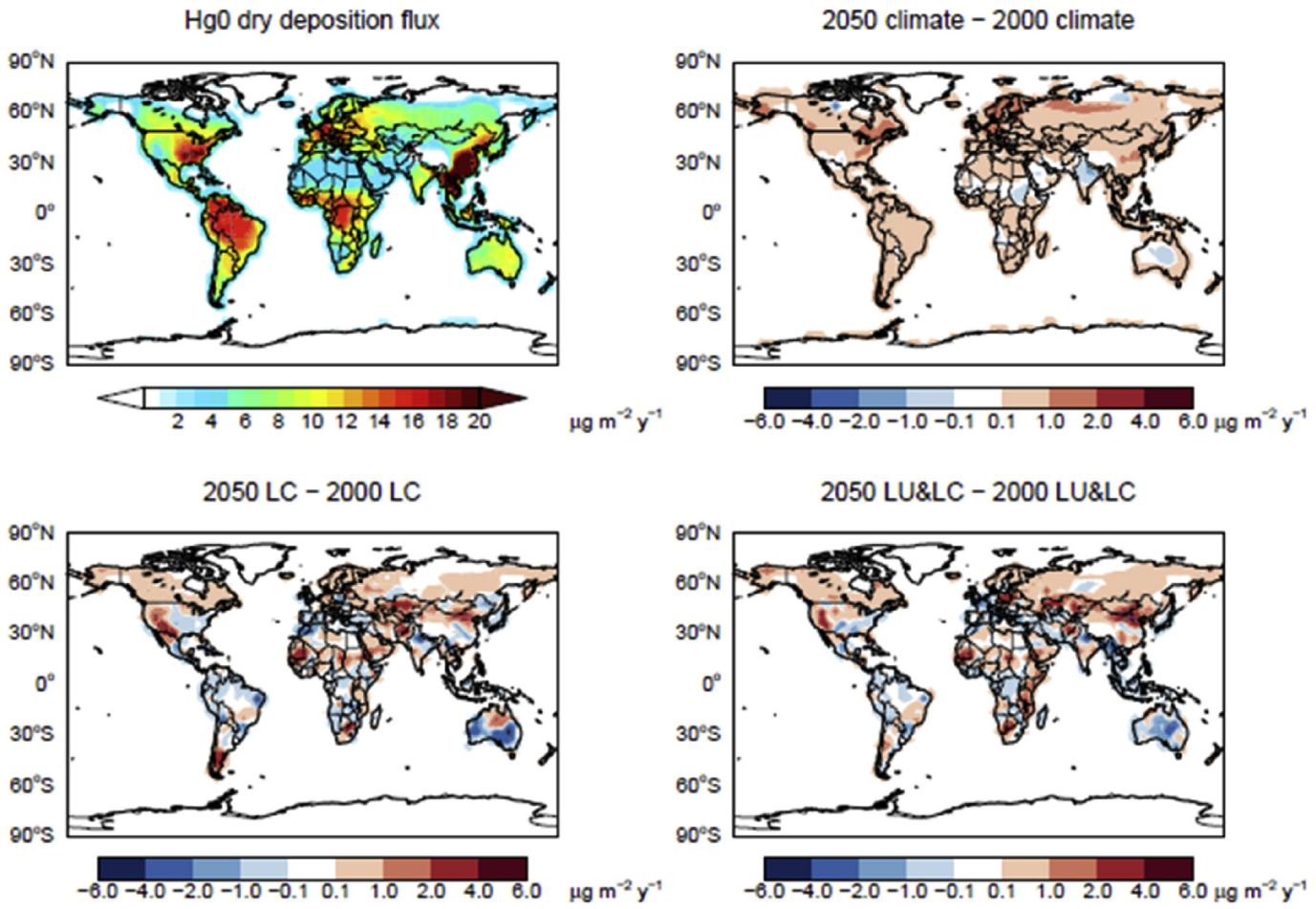

Fig. 7. Annual mean Hg(0) dry deposition flux for the present-day (top left) and the impacts from 2000 to 2050 climate change (top right), land cover change (bottom left), and the combined land use/land cover change (bottom right).

North Pacific, North Atlantic and South Atlantic are not significant. Annual mean mercury wet deposition fluxes to the northern and southern high latitude increase by 7% and 8% respectively largely driven by the increase in precipitation. The annual total precipitation increases by 21% and 11% respectively.

We further examine the impacts of changes in climate and land use/land cover on the gross deposition of mercury (dry deposition, wet deposition plus sea salt uptake of gaseous Hg(II)). Fig. 9 shows the model calculated annual mean gross mercury deposition flux for the present-day and the perturbations due to 2000–2050 changes in climate, natural vegetation and agricultural land use. Climate change leads to general increases in gross deposition flux over the continental regions and decreases over most of the ocean areas in the northern hemisphere, mainly following the changes in mercury wet deposition as discussed above. Specifically, we find annual mean gross mercury deposition flux increases by 3% 3%, 4%, 4% and 3% in North America, Asia, Africa, South America and Australia, respectively and these changes are statistically significant at the 95% confidence level. No significant changes are found in Europe. The annual mean gross mercury deposition flux is only found to decrease significantly by 5% in the Middle Atlantic Ocean basin while no significant changes are found in the North Pacific, North Atlantic, South Atlantic, northern and southern high latitudes. Our results here for the northern high latitudes are different from Hansen et al. (2015) which followed SRES A1B (Nakicenovic et al., 2000) for future climate (2090–2100) Hg simulation using a different Hg model. Hansen et al. (2015) found that the total deposition of Hg to the Arctic Circle (66.5°N) was significantly lower (18%) in the future climate than the present-day climate, mainly due to the lower RGM air concentrations. In response to the 2000–2050 changes in land use/land cover, the gross deposition of mercury is projected to increase over most continental regions but decrease over oceans. This implies that, due to the enhanced uptake of mercury associated with denser vegetation in the 2050s, a larger fraction of mercury would be accumulated in the terrestrial reservoir rather than the ocean reservoir. This has significant implications for policies as atmospheric deposition of mercury serves as the dominant source of mercury inputs to open ocean regions (Mason and Sheu, 2002; Soerensen et al., 2010; Sunderland and Mason, 2007).

3.4. Effects on the global and regional mercury budget

Table 1a and Table 1b show the global and regional total Hg(0) dry deposition and total wet deposition of gaseous and particulate phase Hg(II). Climate change impacts global mercury cycling through different channels. First of all, climate change could impact the air-surface exchange process. We find that climate change causes Hg(0) dry deposition to increase significantly in most of the continental regions mainly driven by the increase in surface Hg(0) concentration. The global total uptake of mercury by sea salt aerosols is found to decrease by 8% (not shown in the table), mainly

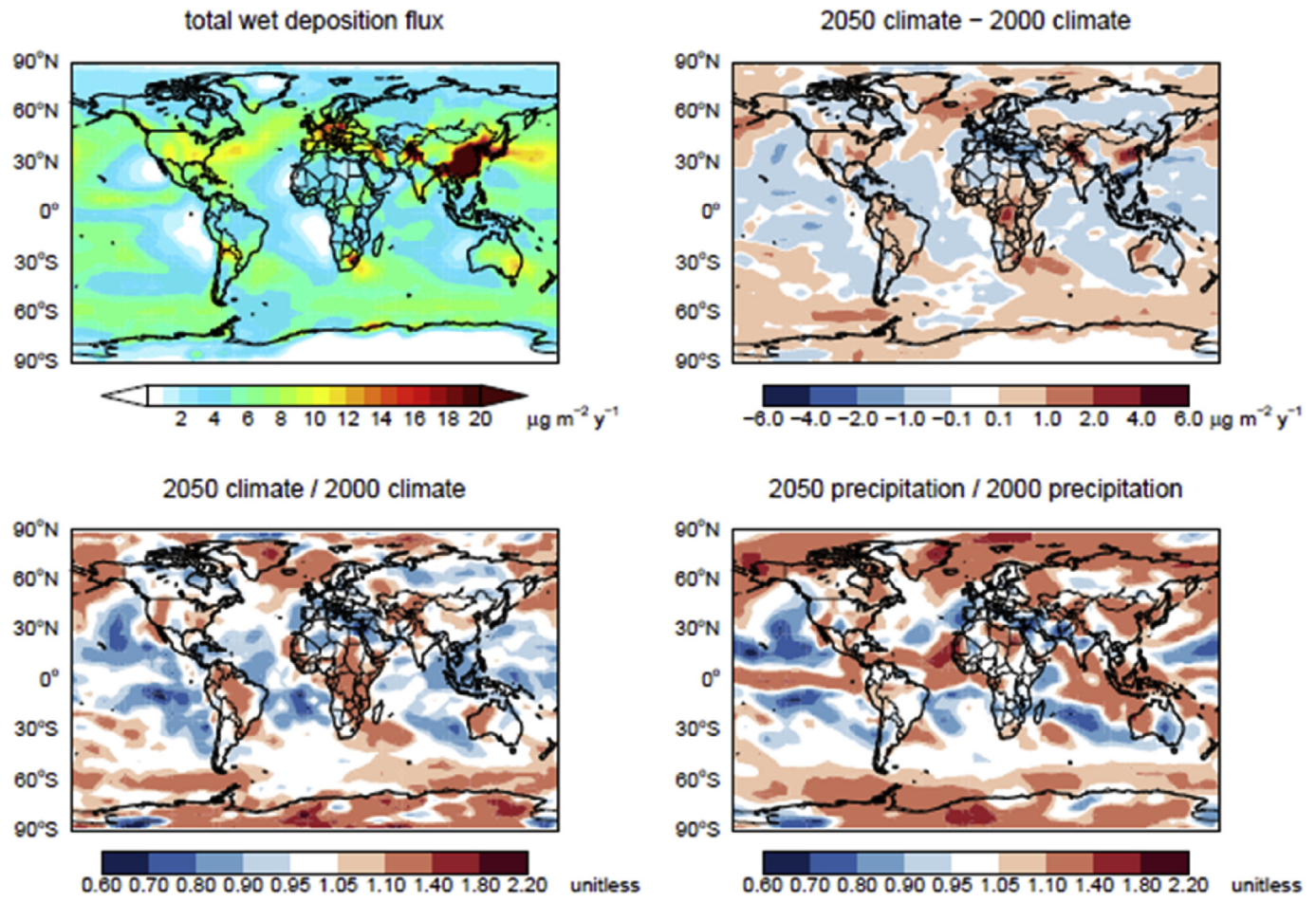

Fig. 8. Annual mean total wet deposition flux for the present-day (top left) and the difference due to 2000–2050 climate change (top right), the ratio due to 2000–2050 climate change (bottom left), annual mean total surface precipitation ratio due to 2000–2050 climate change (bottom right).

driven by the decrease in the atmospheric Hg(II) concentration. Total wet deposition is calculated to increase by 5% and 6% in South America and Africa and no significant change is found globally. In addition, climate change potentially influences secondary emission of Hg(0). We find a 9% (not shown in the table) decrease in global mercury emissions from snow, which is mainly due to the decreases in snow cover in a warmer climate. The decrease in re-emission of Hg(0) together with the increase in Hg(0) dry deposition causes the global net emission of Hg(0) from the terrestrial surface in the 2050 climate to decrease by 11%.

Changes in vegetation in the future primarily affect mercury dry deposition over the continental regions. Global total Hg(0) dry deposition is calculated to increase by 3% as a result of combined effects from anthropogenic land use change and natural vegetation changes over the 2000–2050 period. This is largely driven by the increase in LAI, which enhances the vegetation uptake of Hg(0). We also find the 2000–2050 changes in land use and land cover cause the global net emission of Hg(0) to decrease by 9% mainly as a result of the augmentation in Hg(0) dry deposition.

No significant change is found in global ocean evasion in the future climate but significant regional changes are found. Ocean evasion from the Arctic Ocean and Antarctic Ocean increase by 29% and 14% respectively, largely affected by the increase in temperature with increasing by 3.5 K and 1.6 K, respectively. No significant changes are found for the North Pacific Ocean and Atlantic Ocean (North Atlantic + Middle Atlantic + South Atlantic). We note our results here only show partial sensitivity of air-surface ocean exchange to meteorology change such as temperature. Some recent offline global ocean models (Zhang et al., 2014a, 2014b) have been developed to study the anthropogenic influence on mercury levels in the ocean, but have not been coupled to atmospheric chemical transport models. In addition, sea ice cover plays an important role in air-ocean exchange of Hg(0) (Chen et al., 2015; Fisher et al., 2012; Zhang et al., 2015) and it is not explicitly simulated in the model used in this study.

Climate change could affect the atmospheric mercury redox chemistry mainly through the change in temperature. The increase in secondary emission of Hg(0) and the increase in in-cloud reduction of Hg(II) together lead to a 7% increase of global Hg(0) burden as seen in Table 2. Correspondingly, the global average atmospheric lifetime of mercury is calculated to increase by 4% which could have potential effects on the long range transport of mercury.

4. Conclusions

We investigate the potential impacts on atmospheric mercury from 2000 to 2050 changes in climate and land use/land cover by combining a global chemical transport model (GEOS-Chem), a general circulation model (GISS GCM 3), and a global dynamic vegetation model (LPJ).

Our results demonstrate the potential impacts from climate change on atmospheric mercury through different processes. First,

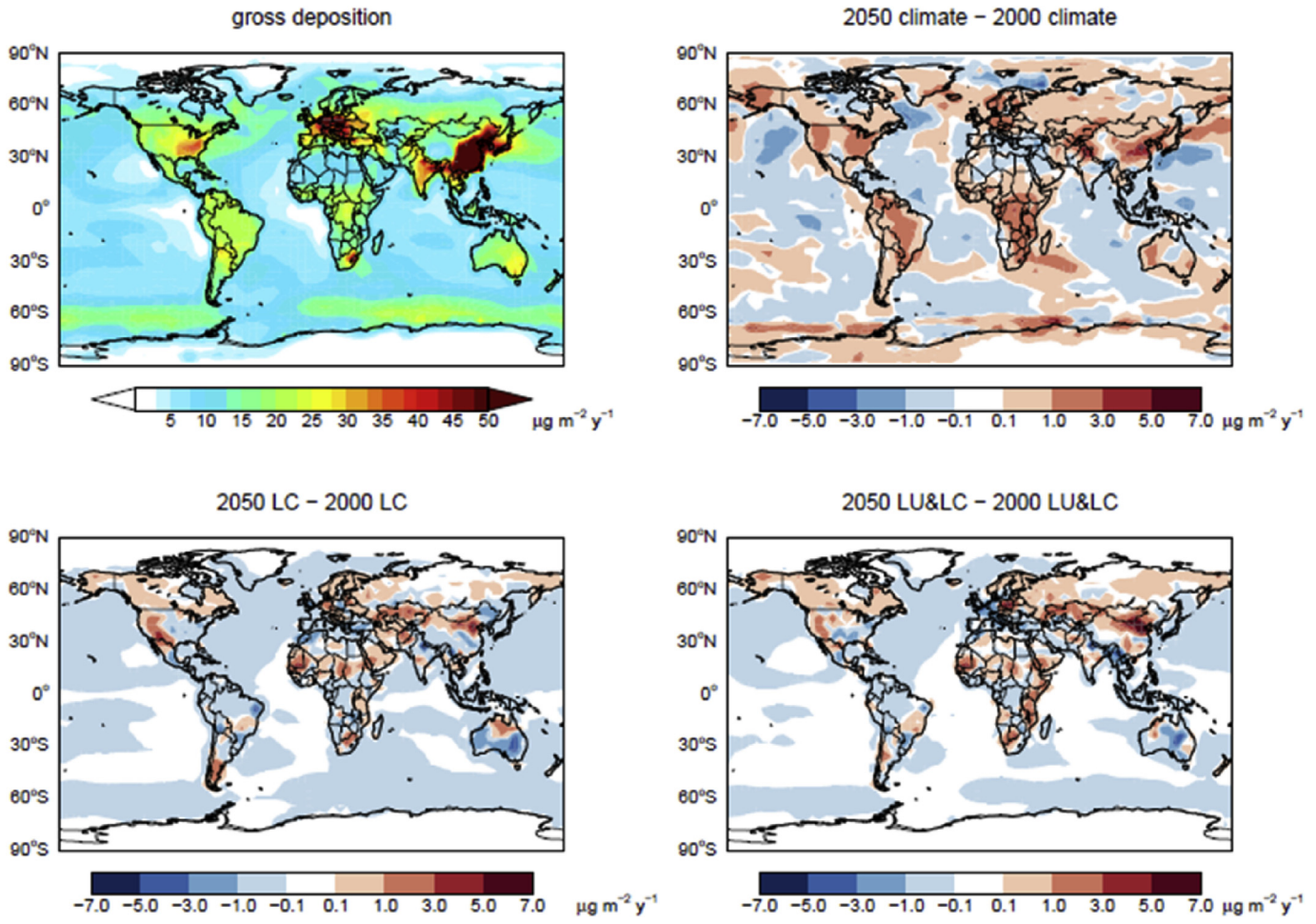

Fig. 9. Same as Fig. 7, but for total (Hg(0) + Hg(II)) mercury deposition flux.

Table 1a
Global and regional total Hg(0) dry deposition for the present-day and the perturbations due to 2000–2050 changes in climate and land use/land cover. The regions are those defined in Sec 3.2.

	2000 Climate + 2000 LU&LC	2050 Climate + 2000 LU&LC	2000 Climate + 2000 LU&LC
North America	161[a]	171 (+6%)[b]	172 (+7%)
Europe	114	123 (+8%)	117 (+3%)
South America	218	224 (+3%)	217
Asia	223	232 (+4%)	236 (+6%)
Africa	261	267	275 (+5%)
global	1440	1508 (+5%)	1480 (+3%)

[a] Units are in Mg/yr.
[b] Numbers in the parentheses are the percent changes at the 95% confidence level and also significant comparing with the respective IAV of present-day.

Table 1b
Same as Table 1a, but for total wet deposition of gaseous and particulate phase Hg(II).

	2000 Climate + 2000 LU&LC	2050 Climate + 2000 LU&LC	2000 Climate + 2000 LU&LC
North America	133	136	131
Europe	95	90	94
South America	100	106 (+6%)	98
Asia	297	307	293
Africa	167	176 (+5%)	166
global	2918	2947	2882

the future changes in precipitation have important implications for the spatial distribution of total mercury wet deposition. Atmospheric mercury redox chemistry is also affected by climate change through changes in temperature and cloud water with global mercury reduction increasing by 5%. The increase in atmospheric mercury reduction together with suppressed Hg(0) oxidation cause

Table 2
Global atmospheric Hg(0) burden, oxidation and reduction of mercury, and atmospheric lifetime of mercury for the present-day and the perturbations due to 2000–2050 changes in climate and land use/land cover.

	2000 Climate + 2000 LU&LC	2050 Climate + 2000 LU&LC	2000 Climate + 2050 LU&LC
Global Hg(0) burden (Mg yr^{-1})	3990	4260 (+7%)[a]	3940
Gross oxidation of Hg(0)	5857	5921	5783
Gross reduction of Hg(II)	1839	1925 (+5%)	1815
Atmospheric lifetime of mercury (yr)	0.78	0.81 (+4%)	0.77

[a] Numbers in the parentheses are the percent changes at the 95% confidence level and also significant comparing with the respective IAV of present-day.

the surface Hg(0) concentration to increase globally with significant changes occuring over most continental regions and ocean regions. As a consequence, the Hg(0) dry deposition flux increases globally. In addition, climate change can significantly affect secondary mercury emissions. Reduced snow coverage causes a 9% global decrease in Hg(0) emissions from snow. The future changes in surface ocean temperature and atmospheric deposition driven by climate change also result in significant changes in atmospheric-surface ocean exchange of atmospheric Hg(0).

Land use and land cover changes lead to general increases in Hg(0) dry deposition flux with large spatial variations. This is largely due to the augmented Hg(0) dry deposition velocity driven by changes in vegetation type and density. We find general increases in the annual mean Hg(0) dry deposition flux in northern mid-latitudes, which reflects the prevailing changes of vegetation. The largest increases in the annual mean Hg(0) dry deposition flux up to 6 $\mu g/m^2/yr$ are found over the western United States, part of North Africa, central Asia and northern China. The global total Hg(0) dry deposition in the 2050s will increase by 3% driven by changes in natural vegetation and anthropogenic land use.

Our results show significant change in surface Hg(0) and gaseous Hg(II) concentrations in the Arctic Ocean driven by future changes in climate. A previous study by Fisher et al. (2013) has shown that the larger interannual variability in atmospheric Hg in several observation sites in the Arctic is driven by environmental factors such as temperature and potentially climate change over the past 30 years. Other studies also suggest the biogeochemical cycling of Hg in the Arctic Ocean is sensitive to ongoing climate variability (Krabbenhoft and Sunderland, 2013; Soerensen et al., 2016; Stern et al., 2012). Our results illustrate the potential effects of future climate change on atmospheric mercury in the Arctic Ocean and the discrepancy between model results in our work and that of Hansen et al. (2015) requires more modeling efforts to reduce the uncertainty.

Our results show that the gross mercury deposition flux could increase over most continental regions driven by changes in 2000–2050 climate and land use/land cover. This implies increased mercury uptake by the terrestrial system which decreases the mobilization of Hg. However, deep ocean and soil reservoirs are not explicitly simulated in our model and we are unable to evaluate the long-term impact on the soil and deep ocean reservoir of mercury. This study does not account for the potential effects on biomass burning emissions of mercury associated with the changes in climate and land use/land cover. Some preliminary results from ongoing research (Kumar et al., 2016) indicate these effects can be significant for some regions. There are also substantial uncertainties associated with the model treatment of air-surface exchange (Selin et al., 2008; Soerensen et al., 2010; Song et al., 2015) and atmospheric chemistry of mercury (Holmes et al., 2006, 2010) as well as the mercury measurements (Jaffe et al., 2014). These uncertainties can significantly affect our projection on the long-term evolution of atmospheric mercury in the coming decades. More mercury measurements and model development efforts are needed to reduce these uncertainties (Gustin et al., 2015).

Acknowledgements

This work was supported by the National Science Foundation (grant #1313755) and U.S. EPA (grant #83518901). We are grateful to Dr. Jed Kaplan (University of Lausanne) for providing the LPJ vegetation data. We thank Dr. Noelle E. Selin (MIT) for helpful discussion on the atmospheric mercury chemistry in the model. We also thank Dr. Anne L. Soerensen (Stockholm University) and Dr. Jenny A. Fisher (University of Wollongong) for helpful discussion on air-ocean exchange of mercury in the model. Superior, a high performance computing cluster at Michigan Technological University, was used in obtaining results presented in this publication.

References

Agnan, Y., Le Dantec, T., Moore, C.W., Edwards, G.C., Obrist, D., 2016. New constraints on terrestrial surface-atmosphere fluxes of gaseous elemental mercury using a global database. Environ. Sci. Technol. 50, 507–524. http://dx.doi.org/10.1021/acs.est.5b04013.

Almeida, M.D., Marins, R.V., Paraquetti, H.H.M., Bastos, W.R., Lacerda, L.D., 2009. Mercury degassing from forested and open field soils in Rondonia, Western Amazon, Brazil. Chemosphere 77, 60–66. http://dx.doi.org/10.1016/j.chemosphere.2009.05.018.

Amos, H.M., Jacob, D.J., Holmes, C.D., Fisher, J.A., Wang, Q., Yantosca, R.M., Corbitt, E.S., Galarneau, E., Rutter, A.P., Gustin, M.S., Steffen, A., Schauer, J.J., Graydon, J.A., St Louis, V.L., Talbot, R.W., Edgerton, E.S., Zhang, Y., Sunderland, E.M., 2012. Gas-particle partitioning of atmospheric Hg(II) and its effect on global mercury deposition. Atmos. Chem. Phys. 12, 591–603. http://dx.doi.org/10.5194/acp-12-591-2012.

Amos, H.M., Jacob, D.J., Streets, D.G., Sunderland, E.M., 2013. Legacy impacts of all-time anthropogenic emissions on the global mercury cycle. Glob. Biogeochem. Cycles 27, 410–421. http://dx.doi.org/10.1002/gbc.20040.

Andersson, M.E., Gardfeldt, K., Wangberg, I., Stromberg, D., 2008. Determination of Henry's law constant for elemental mercury. Chemosphere 73, 587–592. http://dx.doi.org/10.1016/j.chemosphere.2008.05.067.

Bachelet, D., Neilson, R.P., Lenihan, J.M., Drapek, R.J., 2001. Climate change effects on vegetation distribution and carbon budget in the United States. Ecosystems 4, 164–185. http://dx.doi.org/10.1007/s10021-001-0002-7.

Bash, J.O., Bresnahan, P., Miller, D.R., 2007. Dynamic surface interface exchanges of mercury: a review and compartmentalized modeling framework. J. Appl. Meteorol. Climatol. 46, 1606–1618. http://dx.doi.org/10.1175/jam2553.1.

Bash, J.O., 2010. Description and initial simulation of a dynamic bidirectional air-surface exchange model for mercury in Community Multiscale Air Quality (CMAQ) model. J. Geophys. Res. Atmos. 115 http://dx.doi.org/10.1029/2009jd012834.

Bergan, T., Gallardo, L., Rodhe, H., 1999. Mercury in the global troposphere: a three-dimensional model study. Atmos. Environ. 33, 1575–1585. http://dx.doi.org/10.1016/s1352-2310(98)00370-7.

Bey, I., Jacob, D.J., Yantosca, R.M., Logan, J.A., Field, B.D., Fiore, A.M., Li, Q.B., Liu, H.G.Y., Mickley, L.J., Schultz, M.G., 2001. Global modeling of tropospheric chemistry with assimilated meteorology: model description and evaluation. J. Geophys. Res. Atmos. 106, 23073–23095.

Blackwell, B.D., Driscoll, C.T., Maxwell, J.A., Holsen, T.M., 2014. Changing climate alters inputs and pathways of mercury deposition to forested ecosystems. Biogeochemistry 119, 215–228. http://dx.doi.org/10.1007/s10533-014-9961-6.

Chen, L., Zhang, Y., Jacob, D.J., Soerensen, A.L., Fisher, J.A., Horowitz, H.M., Corbitt, E.S., Wang, X., 2015. A decline in Arctic Ocean mercury suggested by differences in decadal trends of atmospheric mercury between the Arctic and northern Midlatitudes. Geophys. Res. Lett. 42, 6076–6083. http://dx.doi.org/10.1002/2015gl064051.

Choi, A.L., Grandjean, P., 2008. Methylmercury exposure and health effects in humans. Environ. Chem. 5, 112–120. http://dx.doi.org/10.1071/en08014.

Corbitt, E.S., Jacob, D.J., Holmes, C.D., Streets, D.G., Sunderland, E.M., 2011. Global source-receptor relationships for mercury deposition under present-day and 2050 emissions scenarios. Environ. Sci. Technol. 45, 10477–10484. http://dx.doi.org/10.1021/es202496y.

Cox, P.M., Betts, R.A., Collins, M., Harris, P.P., Huntingford, C., Jones, C.D., 2004. Amazonian forest dieback under climate-carbon cycle projections for the 21st century. Theor. Appl. Climatol. 78, 137–156. http://dx.doi.org/10.1007/s00704-004-0049-4.

Cramer, W., Bondeau, A., Woodward, F.I., Prentice, I.C., Betts, R.A., Brovkin, V., Cox, P.M., Fisher, V., Foley, J.A., Friend, A.D., Kucharik, C., Lomas, M.R., Ramankutty, N., Sitch, S., Smith, B., White, A., Young-Molling, C., 2001. Global response of terrestrial ecosystem structure and function to CO2 and climate change: results from six dynamic global vegetation models. Glob. Change Biol. 7, 357–373. http://dx.doi.org/10.1046/j.1365-2486.2001.00383.x.

Eckley, C.S., Branfireun, B., 2008. Gaseous mercury emissions from urban surfaces: controls and spatiotemporal trends. Appl. Geochem. 23, 369–383. http://dx.doi.org/10.1016/j.apgeochem.2007.12.008.

Ericksen, J.A., Gustin, M.S., Schorran, D.E., Johnson, D.W., Lindberg, S.E., Coleman, J.S., 2003. Accumulation of atmospheric mercury in forest foliage. Atmos. Environ. 37, 1613–1622. http://dx.doi.org/10.1016/s1352-2310(03)00008-6.

Ericksen, J.A., Gustin, M.S., 2004. Foliar exchange of mercury as a function of soil and air mercury concentrations. Sci. Total Environ. 324, 271–279. http://dx.doi.org/10.1016/j.scitotenv.200310.034.

Ericksen, J.A., Gustin, M.S., Xin, M., Weisberg, P.J., Fernandez, G.C.J., 2006. Air-soil exchange of mercury from background soils in the United States. Sci. Total Environ. 366, 851–863. http://dx.doi.org/10.1016/j.scitotenv.2005.08.019.

Fain, X., Grangeon, S., Bahlmann, E., Fritsche, J., Obrist, D., Dommergue, A., Ferrari, C.P., Cairns, W., Ebinghaus, R., Barbante, C., Cescon, P., Boutron, C., 2007. Diurnal production of gaseous mercury in the alpine snowpack before snowmelt. J. Geophys. Res. Atmos. 112 http://dx.doi.org/10.1029/2007jd008520.

Fain, X., Ferrari, C.P., Dommergue, A., Albert, M., Battle, M., Arnaud, L., Barnola, J.M., Cairns, W., Barbante, C., Boutron, C., 2008. Mercury in the snow and firn at Summit Station, Central Greenland, and implications for the study of past atmospheric mercury levels. Atmos. Chem. Phys. 8, 3441–3457.

Fisher, J.A., Jacob, D.J., Soerensen, A.L., Amos, H.M., Steffen, A., Sunderland, E.M., 2012. Riverine source of Arctic Ocean mercury inferred from atmospheric observations. Nat. Geosci. 5, 499–504. http://dx.doi.org/10.1038/ngeo1478.

Fisher, J.A., Jacob, D.J., Soerensen, A.L., Amos, H.M., Corbitt, E.S., Streets, D.G., Wang, Q., Yantosca, R.M., Sunderland, E.M., 2013. Factors driving mercury variability in the Arctic atmosphere and ocean over the past 30 years. Glob. Biogeochem. Cycles 27, 1226–1235. http://dx.doi.org/10.1002/2013gb004689.

Fu, X., Feng, X., Sommar, J., Wang, S., 2012a. A review of studies on atmospheric mercury in China. Sci. Total Environ. 421, 73–81. http://dx.doi.org/10.1016/j.scitotenv.2011.09.089.

Fu, X., Feng, X., Zhang, H., Yu, B., Chen, L., 2012b. Mercury emissions from natural surfaces highly impacted by human activities in Guangzhou province, South China. Atmos. Environ. 54, 185–193. http://dx.doi.org/10.1016/j.atmosenv.2012.02.008.

Ganzeveld, L., Bouwman, L., Stehfest, E., van Vuuren, D.P., Eickhout, B., Lelieveld, J., 2010. Impact of future land use and land cover changes on atmospheric chemistry-climate interactions. J. Geophys. Res. Atmos. 115 http://dx.doi.org/10.1029/2010jd014041.

Gao, W., Wesely, M.L., 1995. Modeling gaseous dry deposition over regional scales with satellite-observations .1. Model development. Atmos. Environ. 29, 727–737. http://dx.doi.org/10.1016/1352-2310(94)00284-r.

Gratz, L.E., Keeler, G.J., Miller, E.K., 2009. Long-term relationships between mercury wet deposition and meteorology. Atmos. Environ. 43, 6218–6229. http://dx.doi.org/10.1016/j.atmosenv.2009.08.040.

Gustin, M.S., Engle, M., Ericksen, J., Lyman, S., Stamenkovic, J., Xin, M., 2006. Mercury exchange between the atmosphere and low mercury containing substrates. Appl. Geochem. 21, 1913–1923. http://dx.doi.org/10.1016/j.apgeochem.2006.08.007.

Gustin, M.S., Lindberg, S.E., Weisberg, P.J., 2008. An update on the natural sources and sinks of atmospheric mercury. Appl. Geochem. 23, 482–493. http://dx.doi.org/10.1016/j.apgeochem.2007.12.010.

Gustin, M.S., Amos, H.M., Huang, J., Miller, M.B., Heidecorn, K., 2015. Measuring and modeling mercury in the atmosphere: a critical review. Atmos. Chem. Phys. 15, 5697–5713. http://dx.doi.org/10.5194/acp-15-5697-2015.

Hansen, K.M., Christensen, J.H., Brandt, J., 2015. The influence of climate change on atmospheric deposition of mercury in the arctic-a model sensitivity study. Int. J. Environ. Res. Public Health 12, 11254–11268. http://dx.doi.org/10.3390/ijerph120911254.

Hanson, P.J., Lindberg, S.E., Tabberer, T.A., Owens, J.G., Kim, K.H., 1995. Foliar exchange of mercury-vapor - evidence for a compensation point. Water Air Soil Pollut. 80, 373–382. http://dx.doi.org/10.1007/bf01189687.

Hartman, J.S., Weisberg, P.J., Pillai, R., Ericksen, J.A., Kuiken, T., Lindberg, S.E., Zhang, H., Rytuba, J.J., Gustin, M.S., 2009. Application of a rule-based model to estimate mercury exchange for three background biomes in the continental United States. Environ. Sci. Technol. 43, 4989–4994. http://dx.doi.org/10.1021/es900075q.

Holmes, C.D., Jacob, D.J., Yang, X., 2006. Global lifetime of elemental mercury against oxidation by atomic bromine in the free troposphere. Geophys. Res. Lett. 33 http://dx.doi.org/10.1029/2006gl027176.

Holmes, C.D., Jacob, D.J., Corbitt, E.S., Mao, J., Yang, X., Talbot, R., Slemr, F., 2010. Global atmospheric model for mercury including oxidation by bromine atoms. Atmos. Chem. Phys. 10, 12037–12057. http://dx.doi.org/10.5194/acp-10-12037-2010.

Holmes, C.D., Krishnamurthy, N.P., Caffrey, J.M., Landing, W.M., Edgerton, E.S., Knapp, K.R., Nair, U.S., 2016. Thunderstorms increase mercury wet deposition. Environ. Sci. Technol. (submitted).

Hossaini, R., Mantle, H., Chipperfield, M.P., Montzka, S.A., Hamer, P., Ziska, E., Quack, B., Krueger, K., Tegtmeier, S., Atlas, E., Sala, S., Engel, A., Boenisch, H., Keber, T., Oram, D., Mills, G., Ordonez, C., Saiz-Lopez, A., Warwick, N., Liang, Q., Feng, W., Moore, E., Miller, B.R., Marecal, V., Richards, N.A.D., Dorf, M., Pfeilsticker, K., 2013. Evaluating global emission inventories of biogenic bromocarbons. Atmos. Chem. Phys. 13, 11819–11838. http://dx.doi.org/10.5194/acp-13-11819-2013.

Houghton, R.A., Skole, D.L., Nobre, C.A., Hackler, J.L., Lawrence, K.T., Chomentowski, W.H., 2000. Annual fluxes or carbon from deforestation and regrowth in the Brazilian Amazon. Nature 403, 301–304. http://dx.doi.org/10.1038/35002062.

Hughes, C., Johnson, M., von Glasow, R., Chance, R., Atkinson, H., Souster, T., Lee, G.A., Clarke, A., Meredith, M., Venables, H.J., Turner, S.M., Malin, G., Liss, P.S., 2012. Climate-induced change in biogenic bromine emissions from the Antarctic marine biosphere. Glob. Biogeochem. Cycles 26. http://dx.doi.org/10.1029/2012gb004295.

IMAGE-Team, 2001. The IMAGE 2.2 implementation of the SRES scenarios. In: A Comprehensive Analysis of Emissions, Climate Change and Impacts in the 21st Century. RIVM CD-ROM Publication 481508018, Bilthoven, the Netherlands, 500110001.

IPCC, 2001. In: Houghton, J.T., Ding, Y., Griggs, D.J., Noguer, M., van der Linden, P.J., Dai, X., Maskell, K., Johnson, C.A. (Eds.), Climate Change 2001: the Scientific Basis, Contribution of Working Group I to the Third Assessment Report of the Intergovernmental Panel on Climate Change, IPCC. Cambridge University Press, Cambridge, United Kingdom and New York, NY, USA, p. 881.

Jaffe, D.A., Lyman, S., Amos, H.M., Gustin, M.S., Huang, J., Selin, N.E., Levin, L., ter Schure, A., Mason, R.P., Talbot, R., Rutter, A., Finley, B., Jaegle, L., Shah, V., McClure, C., Arnbrose, J., Gratz, L., Lindberg, S., Weiss-Penzias, P., Sheu, G.-R., Feddersen, D., Horvat, M., Dastoor, A., Hynes, A.J., Mao, H., Sonke, J.E., Slemr, F., Fisher, J.A., Ebinghaus, R., Zhang, Y., Edwards, G., 2014. Progress on understanding atmospheric mercury hampered by uncertain measurements. Environ. Sci. Technol. 48, 7204–7206. http://dx.doi.org/10.1021/es5026432.

Krabbenhoft, D.P., Sunderland, E.M., 2013. Global change and mercury. Science 341, 1457–1458. http://dx.doi.org/10.1126/science.1242838.

Kumar, A., Wu, S., Huang, Y., 2016. Impacts of Present-2050 Land Cover Change on Hg Wildfire Emissions (submitted).

Lei, H., Wuebbles, D.J., Liang, X.Z., Tao, Z., Olsen, S., Artz, R., Ren, X., Cohen, M., 2014. Projections of atmospheric mercury levels and their effect on air quality in the United States. Atmos. Chem. Phys. 14, 783–795. http://dx.doi.org/10.5194/acp-14-783-2014.

Lin, C.-J., Pongprueksa, P., Lindberg, S.E., Pehkonen, S.O., Byun, D., Jang, C., 2006. Scientific uncertainties in atmospheric mercury models I: model science evaluation. Atmos. Environ. 40, 2911–2928. http://dx.doi.org/10.1016/j.atmosenv.2006.01.009.

Lindberg, S., Bullock, R., Ebinghaus, R., Engstrom, D., Feng, X., Fitzgerald, W., Pirrone, N., Prestbo, E., Seigneur, C., 2007. A synthesis of progress and uncertainties in attributing the sources of mercury in deposition. Ambio 36, 19–32.

Lindqvist, O., Rodhe, H., 1985. Atmospheric mercury - a review. Tellus Ser. B Chem. Phys. Meteorol. 37, 136–159.

Liu, H.Y., Jacob, D.J., Bey, I., Yantosca, R.M., 2001. Constraints from Pb-210 and Be-7 on wet deposition and transport in a global three-dimensional chemical tracer model driven by assimilated meteorological fields. J. Geophys. Res. Atmos. 106, 12109–12128. http://dx.doi.org/10.1029/2000jd900839.

Mason, R., 2009. In: Mason, R., Pirrone, N. (Eds.), Mercury Emissions from Natural Processes and Their Importance in the Global Mercury Cycle, Mercury Fate and Transport in the Global Atmosphere. Springer, US, NewYork, NY, USA, pp. 173–191.

Mason, R.P., Sheu, G.R., 2002. Role of the ocean in the global mercury cycle. Glob. Biogeochem. Cycles 16. http://dx.doi.org/10.1029/2001gb001440.

Megaritis, A.G., Murphy, B.N., Racherla, P.N., Adams, P.J., Pandis, S.N., 2014. Impact of climate change on mercury concentrations and deposition in the eastern United States. Sci. Total Environ. 487, 299–312. http://dx.doi.org/10.1016/j.scitotenv.2014.03.084.

Mergler, D., Anderson, H.A., Chan, L.H.M., Mahaffey, K.R., Murray, M., Sakamoto, M., Stern, A.H., 2007. Methylmercury exposure and health effects in humans: a worldwide concern. Ambio 36, 3–11.

MNP, 2006. In: Bouwman, A.F., Kram, T., Klein Goldewijk, K. (Eds.), Integrated Modelling of Global Environmental Change, an Overview of IMAGE 2.4. Netherlands Environmental Assessment Agency (MNP), Bilthoven, The Netherlands.

NADP, 2009. National Atmospheric Deposition Program: Mercury Deposition Network (MDN): a NADP Network available at: http://nadp.sws.uiuc.edu/MDN/.

Nair, U.S., Wu, Y., Holmes, C.D., Ter Schure, A., Kallos, G., Walters, J.T., 2013. Cloud-resolving simulations of mercury scavenging and deposition in thunderstorms. Atmos. Chem. Phys. 13, 10143–10157. http://dx.doi.org/10.5194/acp-13-10143-2013.

Nakicenovic, N., Alcamo, J., Davis, G., de Vries, B., Fenhann, J., Gaffin, S., Gregory, K., Grbler, A., Jung, T., Kram, T., 2000. Special report on emission scenarios: a special report of working group III of the intergovernmental panel on climate change. In: Special Report on Emissions Scenarios. Academic Publishing, New York, NY, USA.

Nightingale, P.D., Malin, G., Law, C.S., Watson, A.J., Liss, P.S., Liddicoat, M.I., Boutin, J.,

Upstill-Goddard, R.C., 2000. In situ evaluation of air-sea gas exchange parameterizations using novel conservative and volatile tracers. Glob. Biogeochem. Cycles 14, 373–387. http://dx.doi.org/10.1029/1999gb900091.
Obrist, D., Conen, F., Vogt, R., Siegwolf, R., Alewell, C., 2006. Estimation of Hg-0 exchange between ecosystems and the atmosphere using Rn-222 and Hg-0 concentration changes in the stable nocturnal boundary layer. Atmos. Environ. 40, 856–866. http://dx.doi.org/10.1016/j.atmosenv.2005.10.012.
Pacyna, E.G., Pacyna, J.M., Sundseth, K., Munthe, J., Kindbom, K., Wilson, S., Steenhuisen, F., Maxson, P., 2010. Global emission of mercury to the atmosphere from anthropogenic sources in 2005 and projections to 2020. Atmos. Environ. 44, 2487–2499. http://dx.doi.org/10.1016/j.atmosenv.2009.06.009.
Parrella, J.P., Jacob, D.J., Liang, Q., Zhang, Y., Mickley, L.J., Miller, B., Evans, M.J., Yang, X., Pyle, J.A., Theys, N., Van Roozendael, M., 2012. Tropospheric bromine chemistry: implications for present and pre-industrial ozone and mercury. Atmos. Chem. Phys. 12, 6723–6740. http://dx.doi.org/10.5194/acp-12-6723-2012.
Pirrone, N., Cinnirella, S., Feng, X., Finkelman, R.B., Friedli, H.R., Leaner, J., Mason, R., Mukherjee, A.B., Stracher, G.B., Streets, D.G., Telmer, K., 2010. Global mercury emissions to the atmosphere from anthropogenic and natural sources. Atmos. Chem. Phys. 10, 5951–5964. http://dx.doi.org/10.5194/acp-10-5951-2010.
Poissant, L., Pilote, M., Casimir, A., 1999. Mercury flux measurements in a naturally enriched area: correlation with environmental conditions during the Nevada Study and Tests of the Release of Mercury from Soils (STORMS). J. Geophys. Res. Atmos. 104, 21845–21857. http://dx.doi.org/10.1029/1999jd900092.
Poissant, L., Amyot, M., Pilote, M., Lean, D., 2000. Mercury water-air exchange over the upper st. Lawrence river and lake ontario. Environ. Sci. Technol. 34, 3069–3078. http://dx.doi.org/10.1021/es990719a.
Pongprueksa, P., Lin, C.-J., Lindberg, S.E., Jang, C., Braverman, T., Bullock Jr., O.R., Ho, T.C., Chu, H.-W., 2008. Scientific uncertainties in atmospheric mercury models III: boundary and initial conditions, model grid resolution, and Hg(II) reduction mechanism. Atmos. Environ. 42, 1828–1845. http://dx.doi.org/10.1016/j.atmosenv.2007.11.020.
Prestbo, E.M., Gay, D.A., 2009. Wet deposition of mercury in the US and Canada, 1996-2005: results and analysis of the NADP mercury deposition network (MDN). Atmos. Environ. 43, 4223–4233. http://dx.doi.org/10.1016/j.atmosenv.2009.05.028.
Rind, D., Lerner, J., Jonas, J., McLinden, C., 2007. Effects of resolution and model physics on tracer transports in the NASA Goddard Institute for Space Studies general circulation models. J. Geophys. Res. Atmos. 112 http://dx.doi.org/10.1029/2006jd007476.
Risch, M.R., DeWild, J.F., Krabbenhoft, D.P., Kolka, R.K., Zhang, L., 2012a. Litterfall mercury dry deposition in the eastern USA. Environ. Pollut. 161, 284–290. http://dx.doi.org/10.1016/j.envpol.2011.06.005.
Risch, M.R., Gay, D.A., Fowler, K.K., Keeler, G.J., Backus, S.M., Blanchard, P., Barres, J.A., Dvonch, J.T., 2012b. Spatial patterns and temporal trends in mercury concentrations, precipitation depths, and mercury wet deposition in the North American Great Lakes region, 2002-2008. Environ. Pollut. 161, 261–271. http://dx.doi.org/10.1016/j.envpol.2011.05.030.
Rutter, A.P., Schauer, J.J., 2007a. The effect of temperature on the gas-particle partitioning of reactive mercury in atmospheric aerosols. Atmos. Environ. 41, 8647–8657. http://dx.doi.org/10.1016/j.atmosenv.2007.07.024.
Rutter, A.P., Schauer, J.J., 2007b. The impact of aerosol composition on the particle to gas partitioning of reactive mercury. Environ. Sci. Technol. 41, 3934–3939. http://dx.doi.org/10.1021/es062439i.
Rutter, A.P., Schauer, J.J., Shafer, M.M., Creswell, J.E., Olson, M.R., Robinson, M., Collins, R.M., Parman, A.M., Katzman, T.L., Mallek, J.L., 2011. Dry deposition of gaseous elemental mercury to plants and soils using mercury stable isotopes in a controlled environment. Atmos. Environ. 45, 848–855. http://dx.doi.org/10.1016/j.atmosenv.2010.11.025.
Scheulhammer, A.M., Meyer, M.W., Sandheinrich, M.B., Murray, M.W., 2007. Effects of environmental methylmercury on the health of wild birds, mammals, and fish. Ambio 36, 12–18. http://dx.doi.org/10.1579/0044-7447(2007)36[12:eoe-mot]2.0.co;2.
Schroeder, W.H., Munthe, J., 1998. Atmospheric mercury - an overview. Atmos. Environ. 32, 809–822. http://dx.doi.org/10.1016/s1352-2310(97)00293-8.
Seigneur, C., Vijayaraghavan, K., Lohman, K., Karamchandani, P., Scott, C., 2004. Global source attribution for mercury deposition in the United States. Environ. Sci. Technol. 38, 555–569. http://dx.doi.org/10.1021/es034109t.
Selin, N.E., Jacob, D.J., Park, R.J., Yantosca, R.M., Strode, S., Jaegle, L., Jaffe, D., 2007. Chemical cycling and deposition of atmospheric mercury: global constraints from observations. J. Geophys. Res. Atmos. 112 http://dx.doi.org/10.1029/2006jd007450.
Selin, N.E., Jacob, D.J., 2008. Seasonal and spatial patterns of mercury wet deposition in the United States: constraints on the contribution from North American anthropogenic sources. Atmos. Environ. 42, 5193–5204. http://dx.doi.org/10.1016/j.atmosenv.2008.02.069.
Selin, N.E., Jacob, D.J., Yantosca, R.M., Strode, S., Jaegle, L., Sunderland, E.M., 2008. Global 3-D land-ocean-atmosphere model for mercury: present-day versus preindustrial cycles and anthropogenic enrichment factors for deposition (vol. 22, artn no GB3099, 2008). Glob. Biogeochem. Cycles 22. http://dx.doi.org/10.1029/2008gb003282.
Selin, N.E., 2009. Global biogeochemical cycling of mercury: a review. Annu. Rev. Environ. Resour. 34, 43–63. http://dx.doi.org/10.1146/annurev.environ.051308.084314.
Selin, N.E., 2014. Global change and mercury cycling: challenges for implementing a global mercury treaty. Environ. Toxicol. Chem. 33, 1202–1210. http://dx.doi.org/10.1002/etc.2374.
Shia, R.L., Seigneur, C., Pai, P., Ko, M., Sze, N.D., 1999. Global simulation of atmospheric mercury concentrations and deposition fluxes. J. Geophys. Res. Atmos. 104, 23747–23760. http://dx.doi.org/10.1029/1999jd900354.
Sitch, S., Smith, B., Prentice, I.C., Arneth, A., Bondeau, A., Cramer, W., Kaplan, J.O., Levis, S., Lucht, W., Sykes, M.T., Thonicke, K., Venevsky, S., 2003. Evaluation of ecosystem dynamics, plant geography and terrestrial carbon cycling in the LPJ dynamic global vegetation model. Glob. Change Biol. 9, 161–185. http://dx.doi.org/10.1046/j.1365-2486.2003.00569.x.
Soerensen, A.L., Sunderland, E.M., Holmes, C.D., Jacob, D.J., Yantosca, R.M., Skov, H., Christensen, J.H., Strode, S.A., Mason, R.P., 2010. An improved global model for air-sea exchange of mercury: high concentrations over the north atlantic. Environ. Sci. Technol. 44, 8574–8580. http://dx.doi.org/10.1021/es102032g.
Soerensen, A.L., Mason, R.P., Balcom, P.H., Sunderland, E.M., 2013. Drivers of surface ocean mercury concentrations and air-sea exchange in the west Atlantic Ocean. Environ. Sci. Technol. 47, 7757–7765. http://dx.doi.org/10.1021/es401354q.
Soerensen, A.L., Mason, R.P., Balcom, P.H., Jacob, D.J., Zhang, Y., Kuss, J., Sunderland, E.M., 2014. Elemental mercury concentrations and fluxes in the tropical atmosphere and ocean. Environ. Sci. Technol. 48, 11312–11319. http://dx.doi.org/10.1021/es503109p.
Soerensen, A.L., Jacob, D.J., Schartup, A.T., Fisher, J.A., Lehnherr, I., Louis, V.L.S., Heimbürger, L.-E., Sonke, J.E., Krabbenhoft, D.P., Sunderland, E.M., 2016. A mass budget for mercury and methylmercury in the Arctic Ocean. Glob. Biogeochem. Cycles 30, 560–575. http://dx.doi.org/10.1002/2015GB005280.
Song, S., Selin, N.E., Soerensen, A.L., Angot, H., Artz, R., Brooks, S., Brunke, E.G., Conley, G., Dommergue, A., Ebinghaus, R., Holsen, T.M., Jaffe, D.A., Kang, S., Kelley, P., Luke, W.T., Magand, O., Marumoto, K., Pfaffhuber, K.A., Ren, X., Sheu, G.R., Slemr, F., Warneke, T., Weigelt, A., Weiss-Penzias, P., Wip, D.C., Zhang, Q., 2015. Top-down constraints on atmospheric mercury emissions and implications for global biogeochemical cycling. Atmos. Chem. Phys. 15, 7103–7125. http://dx.doi.org/10.5194/acp-15-7103-2015.
Stern, G.A., Macdonald, R.W., Outridge, P.M., Wilson, S., Chetelat, J., Cole, A., Hintelmann, H., Loseto, L.L., Steffen, A., Wang, F., Zdanowicz, C., 2012. How does climate change influence arctic mercury? Sci. Total Environ. 414, 22–42. http://dx.doi.org/10.1016/j.scitotenv.2011.10.039.
Streets, D.G., Zhang, Q., Wu, Y., 2009. Projections of global mercury emissions in 2050. Environ. Sci. Technol. 43, 2983–2988. http://dx.doi.org/10.1021/es802474j.
Strode, S.A., Jaegle, L., Selin, N.E., Jacob, D.J., Park, R.J., Yantosca, R.M., Mason, R.P., Slemr, F., 2007. Air-sea exchange in the global mercury cycle. Glob. Biogeochem. Cycles 21. http://dx.doi.org/10.1029/2006gb002766.
Subir, M., Ariya, P.A., Dastoor, A.P., 2011. A review of uncertainties in atmospheric modeling of mercury chemistry I. Uncertainties in existing kinetic parameters - fundamental limitations and the importance of heterogeneous chemistry. Atmos. Environ. 45, 5664–5676. http://dx.doi.org/10.1016/j.atmosenv.2011.04.046.
Subir, M., Ariya, P.A., Dastoor, A.P., 2012. A review of the sources of uncertainties in atmospheric mercury modeling II. Mercury surface and heterogeneous chemistry - a missing link. Atmos. Environ. 46, 1–10. http://dx.doi.org/10.1016/j.atmosenv.2011.07.047.
Sunderland, E.M., Mason, R.P., 2007. Human impacts on open ocean mercury concentrations. Glob. Biogeochem. Cycles 21. http://dx.doi.org/10.1029/2006gb002876.
Turner, B.L., Meyer, W.B., Skole, D.L., 1994. Global land-use land-cover change - towards an integrated study. Ambio 23, 91–95.
UNEP, 2013. Global Mercury Assessment 2013: Sources, Emissions, Releases and Environmental Transport. UNEP Chemicals Branch, Geneva, Switzerland.
van der Werf, G.R., Randerson, J.T., Giglio, L., Collatz, G.J., Mu, M., Kasibhatla, P.S., Morton, D.C., DeFries, R.S., Jin, Y., van Leeuwen, T.T., 2010. Global fire emissions and the contribution of deforestation, savanna, forest, agricultural, and peat fires (1997-2009). Atmos. Chem. Phys. 10, 11707–11735. http://dx.doi.org/10.5194/acp-10-11707-2010.
Wang, Q., Jacob, D.J., Fisher, J.A., Mao, J., Leibensperger, E.M., Carouge, C.C., Le Sager, P., Kondo, Y., Jimenez, J.L., Cubison, M.J., Doherty, S.J., 2011. Sources of carbonaceous aerosols and deposited black carbon in the Arctic in winter-spring: implications for radiative forcing. Atmos. Chem. Phys. 11, 12453–12473. http://dx.doi.org/10.5194/acp-11-12453-2011.
Wang, X., Lin, C.J., Feng, X., 2014. Sensitivity analysis of an updated bidirectional air-surface exchange model for elemental mercury vapor. Atmos. Chem. Phys. 14, 6273–6287. http://dx.doi.org/10.5194/acp-14-6273-2014.
Wang, Y., Jacob, D.J., Logan, A.J., 1998. Global simulation of tropospheric O3-NOx-hydrocarbon chemistry. 1. Model formulation. J. Geophys. Res. 103, 10713–10725.
Wesely, M.L., 1989. Parameterization of surface resistances to gaseous dry deposition in regional-scale numerical-models. Atmos. Environ. 23, 1293–1304. http://dx.doi.org/10.1016/0004-6981(89)90153-4.
Wilks, D.S., 2006. Hypothesis testing. In: Statistical Methods in the Atmospheric Sciences, second ed. Academic Press, pp. 138–146.
Wu, S., Mickley, L.J., Jacob, D.J., Logan, J.A., Yantosca, R.M., Rind, D., 2007. Why are there large differences between models in global budgets of tropospheric ozone? J. Geophys. Res. Atmos. 112 http://dx.doi.org/10.1029/2006jd007801.
Wu, S., Mickley, L.J., Kaplan, J.O., Jacob, D.J., 2012. Impacts of changes in land use and land cover on atmospheric chemistry and air quality over the 21st century. Atmos. Chem. Phys. 12, 1597–1609. http://dx.doi.org/10.5194/acp-12-1597-

2012.
Xu, X.H., Yang, X.S., Miller, D.R., Helble, J.J., Carley, R.J., 1999. Formulation of bidirectional atmosphere-surface exchanges of elemental mercury. Atmos. Environ. 33, 4345–4355. http://dx.doi.org/10.1016/s1352-2310(99)00245-9.
Zhang, H., Lindberg, S.E., Marsik, F.J., Keeler, G.J., 2001. Mercury air/surface exchange kinetics of background soils of the Tahquamenon River watershed in the Michigan Upper Peninsula. Water Air Soil Pollut. 126, 151–169. http://dx.doi.org/10.1023/a:1005227802306.
Zhang, L., Wright, L.P., Blanchard, P., 2009. A review of current knowledge concerning dry deposition of atmospheric mercury. Atmos. Environ. 43, 5853–5864. http://dx.doi.org/10.1016/j.atmosenv.2009.08.019.
Zhang, L., Blanchard, P., Gay, D.A., Prestbo, E.M., Risch, M.R., Johnson, D., Narayan, J., Zsolway, R., Holsen, T.M., Miller, E.K., Castro, M.S., Graydon, J.A., St Louis, V.L., Dalziel, J., 2012a. Estimation of speciated and total mercury dry deposition at monitoring locations in eastern and central North America. Atmos. Chem. Phys. 12, 4327–4340. http://dx.doi.org/10.5194/acp-12-4327-2012.
Zhang, Y., Jaegle, L., van Donkelaar, A., Martin, R.V., Holmes, C.D., Amos, H.M., Wang, Q., Talbot, R., Artz, R., Brooks, S., Luke, W., Holsen, T.M., Felton, D., Miller, E.K., Perry, K.D., Schmeltz, D., Steffen, A., Tordon, R., Weiss-Penzias, P., Zsolway, R., 2012b. Nested-grid simulation of mercury over North America. Atmos. Chem. Phys. 12, 6095–6111. http://dx.doi.org/10.5194/acp-12-6095-2012.
Zhang, Y., Jaegle, L., 2013. Decreases in mercury wet deposition over the United States during 2004-2010: roles of domestic and global background emission reductions. Atmosphere 4, 113–131. http://dx.doi.org/10.3390/atmos4020113.
Zhang, Y., Jaegle, L., Thompson, L., 2014a. Natural biogeochemical cycle of mercury in a global three-dimensional ocean tracer model. Glob. Biogeochem. Cycles 28, 553–570. http://dx.doi.org/10.1002/2014gb004814.
Zhang, Y., Jaegle, L., Thompson, L., Streets, D.G., 2014b. Six centuries of changing oceanic mercury. Glob. Biogeochem. Cycles 28, 1251–1261. http://dx.doi.org/10.1002/2014gb004939.
Zhang, Y., Jacob, D.J., Dutkiewicz, S., Amos, H.M., Long, M.S., Sunderland, E.M., 2015. Biogeochemical drivers of the fate of riverine mercury discharged to the global and Arctic Oceans. Glob. Biogeochem. Cycles 29, 854–864. http://dx.doi.org/10.1002/2015gb005124.
Zhu, W., Lin, C.-J., Wang, X., Sommar, J., Fu, X., Feng, X., 2016. Global observations and modeling of atmosphere-surface exchange of elemental mercury: a critical review. Atmos. Chem. Phys. 16, 4451–4480. http://dx.doi.org/10.5194/acp-16-4451-2016.